THE EUROPEAN
PHYSICAL JOURNAL C

$D_s^* \to \phi$ helicity form factors and the exclusive weak decays

Shan Cheng[1,2,a] , **Yao-hui Ju**[1,b], **Qin Qin**[3,c], **Fu-sheng Yu**[4,d]

[1] School of Physics and Electronics, Hunan University, Changsha 410082, People's Republic of China
[2] Hunan Provincial Key Laboratory of High-Energy Scale Physics and Applications, Changsha 410082, People's Republic of China
[3] School of Physics, Huazhong University of Science and Technology, Wuhan 430074, People's Republic of China
[4] School of Nuclear Science and Technology, Lanzhou University, Lanzhou 730000, People's Republic of China

Abstract The decay width of the D_s^* meson is dominated by the electromagnetic mode $D_s^* \to D_s\gamma$, and it is thus the longest-lived charged vector meson. In light of this point, we perform the first QCD LCSRs calculation of $D_s^* \to \phi$ helicity form factors and discuss the experiment potential of discovering exclusive D_s^* weak decays. The main result is the partial decay widths, which read as $\Gamma_{D_s^* \to l\nu} = 2.44 \times 10^{-12}$ GeV, $\Gamma_{D_s^* \to \phi l\nu} = (3.28^{+0.82}_{-0.71}) \times 10^{-14}$ GeV, $\Gamma_{D_s^* \to \phi\pi} = (3.81^{+1.52}_{-1.33}) \times 10^{-14}$ GeV and $\Gamma_{D_s^* \to \phi\rho} = (1.16^{+0.42}_{-0.39}) \times 10^{-13}$ GeV. We show that these channels are promising in the near future, serving as the first experimental observation of weak decays of a vector meson, and would open up a new playground for precision test of the standard model.

1 Introduction

The unitarity of Cabibbo–Kobayashi–Maskawa (CKM) matrix is a crucial criterion of the validity of the Standard Model. Besides the well known unitarity triangles, which indicate the orthogonality between different rows and columns, the CKM unitarity can also be tested by the normalization conditions of individual rows and columns. Nowadays the least precisely determinations are

$$|V_{us}|^2 + |V_{cs}|^2 + |V_{ts}|^2 = 1.026 \pm 0.022,$$
$$|V_{cd}|^2 + |V_{cs}|^2 + |V_{cb}|^2 = 1.025 \pm 0.022, \quad (1)$$

whose uncertainties are both dominated by that of $|V_{cs}| = 0.987 \pm 0.011$ [1]. The $|V_{cs}|$ values are typically extracted

[a] e-mail: scheng@hnu.edu.cn (corresponding author)

[b] e-mail: juyaohui@hnu.edu.cn

[c] e-mail: qqin@hust.edu.cn

[d] e-mail: yufsh@lzu.edu.cn

from semileptonic D decays and leptonic D_s decays, and other independent channels, such as weak D_s^* decays, are highly anticipated to reduce the uncertainty.

Weak D_s^* decays can also provide a platform for examining the heavy quark symmetry, which is the foundation of the heavy quark effective theory [2–4]. The heavy quark spin symmetry relates the ground-state pseudoscalar and vector mesons, e.g. $D_{(s)}$ and $D_{(s)}^*$ mesons. It has been checked through the relation between the semileptonic decays $\bar{B} \to D\ell\bar{\nu}$ and $\bar{B} \to D^*\ell\bar{\nu}$ [5–8], where different spin states appear in the final states. The weak $D_s^{*+} \to \phi\ell^+\nu$ decay, together with $D_s^+ \to \phi\ell^+\nu$, will create the first chance to test the heavy quark spin symmetry with heavy mesons in the initial states.

Practically, $D_s^{*\pm}$ might be the first vector meson whose weak decays will be discovered, because it is the longest-lived charged vector meson indicated by the lattice evaluation of the partial width of its dominant decay channel $D_s^* \to D_s\gamma$ [9]. Once the branching ratio of a weak decay channel is measured, it can be used to indirectly determine the total decay width of $D_s^{*\pm}$ with the theoretical calculation of the weak decay width as an input, for which only an experimental upper limit is currently given as $\Gamma_{D_s^*} < 1900$ keV [1]. Meanwhile, the electromagnetic decay width can also be indirectly determined, from which the electromagnetic coupling $g_{D_s^* D_s \gamma}$ can be extracted. This quantity has been studied by various theoretical approaches (see e.g. [10]), but they suffer large uncertainties due to the significant destructive interference between radiations of the photon from the charm quark and from the strange quark, and also between different QCD power corrections. We highlight the recent LCSRs prediction with the complete NLO at twist-1 and twist-2 level [11], the large cancellation between the charm and strange quark contributions are verified and the large result $g_{D_s^* D_s \gamma} = 0.60^{+0.19}_{-0.18}$ is obtained, which is waiting for

the measurement of experiment. From another perspective, the $g_{D_s^* D_s \gamma}$ coupling is very sensitive to different contributions, so the indirect determination from weak $D_s^{*\pm}$ decays will subsequently act as an important benchmark to probe the involved dynamics.

Evaluating the weak D_s^* decays requires the input of the corresponding heavy-to-light form factors, which are basic physical quantities charactering the momentum redistribution of partons after the weak interaction. In this paper we study the $D_s^* \to \phi$ form factors from QCD light-cone sum rules (LCSRs) approach, which has been widely applied to calculate form factors in charmed meson decays [12–18], and this work is its first implementation in a vector-to-vector transition. Different helicity form factors according to explicit polarizations of the weak current and the ϕ meson are calculated. From the small momentum transfer region $0 \le Q^2 \le 0.4\,\text{GeV}^2$ where the LCSRs predictions are reliable, proper parametrization of the form factors is inevitable to extend them to the large region $0.4 \le Q^2 \lesssim 1.2\,\text{GeV}^2$. We employ both the simplified z-series expansion formalism [19] and the two-pole parametrization [20], and it turns out that the parametrization scheme does not bring additional considerable uncertainties. With the helicity form factors, we obtain the partial decay widths of D_s^* weak decays considered here, they are $\Gamma_{D_s^* \to \phi l \nu} = (3.28^{+0.82}_{-0.71}) \times 10^{-14}\,\text{GeV}$, $\Gamma_{D_s^* \to \phi \pi} = (3.81^{+1.52}_{-1.33}) \times 10^{-14}\,\text{GeV}$ and $\Gamma_{D_s^* \to \phi \rho} = (1.16^{+0.42}_{-0.39}) \times 10^{-13}\,\text{GeV}$. These predictions, together with the partial decay width of the leptonic mode $\Gamma_{D_s^* \to l \nu} = 2.44 \times 10^{-12}\,\text{GeV}$, promote the experiments to measure the weak decay of a vector meson with the great potential in the near future. We remark that the main target of this work is to suggest a feasible measurement of weak decay of vector meson, rather than the precise calculation. The accuracy of our prediction of $D_s^* \to \phi$ form factors is up to leading order of strong coupling and twist five of two-particle LCDA of ϕ meson. The contributions form next-to-leading-order (NLO) correction and three-particle LCDAs of ϕ meson could be accomplished for the study of precise examination after the discovery.

2 $D_s^* \to \phi$ helicity form factors

We start with the correlation function

$$F_{\mu a}(q, p_1) = i \int d^4 x\, e^{iq \cdot x} \langle \phi | T\{J_\mu^W(x), J_a^V(0)\} | 0 \rangle. \quad (2)$$

In the rest frame of the heavy meson D_s^*, the vector current $J_a^V = \bar{c} \gamma_a s$ and the weak current $J_\mu^W = \bar{s} \gamma_\mu (1 - \gamma_5) c$ carry momentum p_{1a} and q_μ, respectively, and hence the momentum of ϕ meson is $p_2 = p_1 - q$. The kinematics in our convention is arranged by

$$p_{1a} = \left(m_{D_s^*}, \mathbf{0} \right), \quad p_{2b} = (E_2, \mathbf{p}), \quad q_\mu = (q_0, -\mathbf{p}),$$

$$\epsilon_{1a}(0) = (0, 0, 0, 1), \quad \epsilon_{1a}(\pm) = \frac{1}{\sqrt{2}}(0, \mp 1, -i, 0).$$

$$\epsilon_{2b}(0) = \frac{1}{m_\phi}(|\mathbf{p}|, 0, 0, E_2), \quad \epsilon_{2b}(\pm) = \frac{1}{\sqrt{2}}(0, \mp 1, -i, 0),$$

$$\bar{\epsilon}_\mu(0) = \frac{1}{\sqrt{q^2}}(|\mathbf{p}|, 0, 0, -q_0), \quad \bar{\epsilon}_\mu(\pm) = \frac{1}{\sqrt{2}}(0, \pm 1, -i, 0). \quad (3)$$

We note that the timelike polarisation of leptonic current $\bar{\epsilon}_\mu(t) = (q_0, 0, 0, -|\mathbf{p}|)/\sqrt{q^2} \propto q_\mu$ does not contribute in the semileptonic decaying processes with massless leptons, and the other three polarisations, picking up the spin-one part of the off-shell W boson, satisfy $q^\mu \bar{\epsilon}_\mu = 0$. Further constraints between these variables can be derived from the kinematical analysis of $1 \to 3$ decaying processes, they are

$$2 m_{D_s^*} E_2 = m_{D_s^*}^2 + m_\phi^2 - q^2,$$

$$2 m_{D_s^*} q_0 = m_{D_s^*}^2 - m_\phi^2 + q^2,$$

$$2 m_{D_s^*} |\mathbf{p}| = \sqrt{\lambda(m_{D_s^*}^2, m_\phi^2, q^2)}, \quad (4)$$

with λ being the källén function $\lambda(M_1, M_2, M_3) = M_1^2 + M_2^2 + M_3^2 - 2M_1 M_2 - 2M_1 M_3 - 2M_2 M_3$. Multiplying both sides of Eq. (2) by the polarisation vector of the weak current, we can decompose the correlation function in terms of invariant helicity amplitudes,

$$\bar{\epsilon}^\mu F_{\mu a}(q, p_1) = \sum_{i,j = \mathbf{0}, \pm} \epsilon_{1a,i'}^* F_{ij}(q^2, p_1^2), \quad (5)$$

here the subscripts i, j and $i' = i + j$ denote the polarisation directions of the weak current, ϕ meson and vector current, respectively.

In the view of LCSRs, correlation functions can be formulated in twofold ways, namely, at the quark level and the hadronic level. Firstly, they can be evaluated directly at the quark-gluon level in the Euclidean momenta space. The QCD calculation of Eq. (2) is carried out with negative q^2, and the operator product expansion (OPE) is valid for large energies of the final state vector mesons, which implies a restriction to not too large momentum transfer squared as $0 \le |q^2| \le q_{\text{LCSR,max}}^2$. In this region, the operator product of the c-quark fields in the correlation function can be expanded near the light cone $x^2 \sim 0$ due to the large virtuality, which at leading order reduces to the free quark propagator.

In the QCD evaluation, only the final ϕ meson is on shell so that $p_2^2 = (p_1 - q)^2 = m_\phi^2$. The OPE calculations obtain the Lorentz decomposition in Eq. (5) where each invariant amplitude can be written in a general convolution of hard functions various LCDAs at different twists [21]

$$F_{ij}^{\rm OPE}(q^2, (p_2+q)^2)$$
$$= \sum_t \int_0^1 du\, T_{ij}^{(t)}(u, q^2, (p_2+q)^2)\, \phi^{(t)}(u). \tag{6}$$

The OPE amplitudes is further rewritten in a dispersion integral over the invariant mass of the interpolating heavy meson,

$$F_{ij}^{\rm OPE}(q^2, p_1^2)$$
$$= \frac{1}{\pi} \int_{m_c^2}^\infty ds\, \frac{u^2}{[u^2 m_\phi^2 - q^2 + m_c^2]} \sum_n \frac{{\rm Im}F_{n,ij}^{\rm OPE}(q^2, s)}{u^n [s - p_1^2]^n}, \tag{7}$$

in which $s \equiv s(q^2, u) = \bar{u} m_\phi^2 + (m_c^2 - \bar{u} q^2)/u$. As an example, we present the imaginary parts of the helicity **00** amplitudes truncated to the third power $n \le 3$, they are

$$\frac{1}{\pi} {\rm Im}F_{1,\mathbf{00}}^{\rm OPE}(q^2 < 0, u)$$
$$= \frac{\sqrt{\lambda}\, m_c f_\phi^\perp m_\phi \phi_2^\perp(u)}{2 m_{D_s^*} \sqrt{|q^2|}} + \frac{\sqrt{\lambda}(u m_{D_s^*}^2 + \bar{u} q^2) f_\phi^\parallel \phi_3^\perp(u)}{2 m_{D_s^*} \sqrt{|q^2|}}$$
$$- \frac{\sqrt{\lambda}(m_{D_s^*}^2 - q^2) f_\phi^\parallel \left[\bar{\phi}_2^\parallel(u) - \bar{\phi}_3^\perp(u)\right]}{2 m_{D_s^*} \sqrt{|q^2|}}$$
$$+ \frac{\sqrt{\lambda} f_\phi^\parallel m_\phi^2 \tilde{\psi}_3^\perp(u)}{4 m_{D_s^*} \sqrt{|q^2|}}, \tag{8}$$

$$\frac{1}{\pi} {\rm Im}F_{2,\mathbf{00}}^{\rm OPE}(q^2 < 0, u)$$
$$= - \frac{\sqrt{\lambda}\left[t\lambda + [m_{D_s^*}^2 - q^2 + t m_\phi^2](m_{D_s^*}^2 - m_\phi^2 + q^2)\right]}{4 m_{D_s^*} \sqrt{|q^2|}}$$
$$\cdot f_\phi^\parallel \left(\bar{\phi}_2^\parallel(u) - \bar{\phi}_3^\perp(u)\right)$$
$$- \frac{\sqrt{\lambda}\left[(t+2) m_{D_s^*}^2 - m_\phi^2 - (t-2)q^2\right]}{4 m_{D_s^*} \sqrt{|q^2|}}$$
$$\cdot f_\phi^\parallel m_\phi^2 \left(\bar{\bar{\psi}}_4^\parallel(u) + \bar{\bar{\phi}}_2^\parallel(u) - 2\bar{\bar{\phi}}_3^\perp(u)\right)$$
$$+ \frac{\sqrt{\lambda}\left(m_{D_s^*}^2 - m_\phi^2 + q^2\right)}{4 m_{D_s^*} \sqrt{|q^2|}} m_c f_\phi^\perp m_\phi\, \tilde{\psi}_3^\parallel(u)$$
$$+ \frac{\sqrt{\lambda}\left(m_{D_s^*}^2 - q^2\right)}{8 m_{D_s^*} \sqrt{|q^2|}} f_\phi^\parallel m_\phi^2 \left(\bar{\phi}_4^\parallel(u) - \bar{\phi}_5^\perp(u)\right)$$
$$+ \frac{\sqrt{\lambda}}{2 m_{D_s^*} \sqrt{|q^2|}} m_c f_\phi^\perp m_\phi^3 \left(\bar{\psi}_4^\perp(u) + \bar{\phi}_2^\perp(u) - 2\bar{\phi}_3^\parallel(u)\right)$$
$$- \frac{\sqrt{\lambda}\left(m_{D_s^*}^2 + t m_\phi^2 - q^2\right)}{4 m_{D_s^*} \sqrt{|q^2|}} m_c f_\phi^\perp m_\phi \left(\bar{\psi}_4^\perp(u) - \bar{\phi}_2^\perp(u)\right)$$
$$- \frac{\sqrt{\lambda}\left(u m_{D_s^*}^2 + \bar{u} q^2\right)}{8 m_{D_s^*} \sqrt{|q^2|}} f_\phi^\parallel m_\phi^2 \phi_5^\perp(u)$$

$$- \frac{\sqrt{\lambda}}{16 m_{D_s^*} \sqrt{|q^2|}} f_\phi^\parallel m_\phi^4 \tilde{\psi}_5^\perp(u), \tag{9}$$

$$\frac{1}{\pi} {\rm Im}F_{3,\mathbf{00}}^{\rm OPE}(q^2 < 0, u)$$
$$= - \frac{\lambda^{3/2}}{2 m_{D_s^*} \sqrt{|q^2|}} m_c f_\phi^\perp m_\phi \left(\bar{\bar{\psi}}_4^\perp(u) + \bar{\bar{\phi}}_2^\perp(u) - 2\bar{\bar{\phi}}_3^\parallel(u)\right)$$
$$+ \frac{f_\phi^\parallel m_\phi^2 [\bar{\phi}_4^\parallel(u) - \bar{\phi}_5^\perp(u)]}{4} \left[\frac{m_c^2 \sqrt{\lambda}\left(m_{D_s^*}^2 - q^2\right)}{m_{D_s^*} \sqrt{|q^2|}}\right.$$
$$\left.+ \frac{\sqrt{\lambda}\left[t\lambda + [m_{D_s^*}^2 - q^2 + t m_\phi^2](m_{D_s^*}^2 - m_\phi^2 + q^2)\right]}{2 m_{D_s^*} \sqrt{|q^2|}}\right]$$
$$+ \frac{\sqrt{\lambda}\left[\bar{u} u \lambda - \left(u m_{D_s^*}^2 - \bar{u} u m_\phi^2 + \bar{u} q^2\right)\left(m_{D_s^*}^2 - m_\phi^2 + q^2\right)\right]}{m_{D_s^*} \sqrt{|q^2|}}$$
$$\cdot f_\phi^\parallel m_\phi^2 \left(\bar{\bar{\psi}}_4^\parallel(u) + \bar{\bar{\phi}}_2^\parallel(u) - 2\bar{\bar{\phi}}_3^\perp(u)\right)$$
$$- \frac{\sqrt{\lambda}}{4 m_{D_s^*} \sqrt{|q^2|}} m_c^3 f_\phi^\perp m_\phi^3 \phi_4^\perp(u)$$
$$- \frac{\sqrt{\lambda}\left[u m_{D_s^*}^2 + \bar{u} q^2\right]}{4 m_{D_s^*} \sqrt{|q^2|}} m_c^2 f_\phi^\parallel m_\phi^2 \phi_5^\perp(u)$$
$$- \frac{\sqrt{\lambda}}{8 m_{D_s^*} \sqrt{|q^2|}} f_\phi^\parallel m_\phi^4 m_c^2 \tilde{\psi}_5^\perp(u), \tag{10}$$

where $t = 2u - 1$, $\phi_2^{\perp(\parallel)}$, $\phi_3^{\perp(\parallel)}$, $\tilde{\psi}_3^{\perp(\parallel)}$, $\phi_4^\parallel$, $\psi_4^{\perp(\parallel)}$, $\phi_5^\perp$, $\tilde{\psi}_5^\perp$ are the LCDAs of ϕ meson at different twists [22–24], the auxiliary functions $\bar{\varphi}(u) \equiv \int_0^u du'\varphi(u')$ and $\bar{\bar{\varphi}}(u) \equiv \int_0^u du' \int_0^{u'} du'' \varphi(u'')$ with $\varphi \in \{\phi, \psi\}$ satisfy the boundary conditions $\bar{\phi}(0) = \bar{\phi}(1) = 0$ and $\bar{\bar{\varphi}}(u = 0, 1) = 0$, respectively, and λ refers to the källén function $\lambda(m_{D_s^*}^2, m_\phi^2, q^2)$. The mass and decay constant are $m_{D_s^*} = 2.112\,{\rm GeV}$, $m_\phi = 1.68\,{\rm GeV}$ [1] and $f_{D_s^*} = 0.274\,{\rm GeV}$ [9]. The twist four and twist five LCDAs begin to contribute at the subleading power term ($n = 2$) according to the twist expansion of matrix element from vacuum to ϕ meson state. The imaginary parts of the other helicity amplitudes ($0\pm$, ±0, $\pm\mp$) are listed in appendix B.

When q^2 shifts from deeply negative to positive, the typical distance grows between the two currents in Eq. (2), hence the long-distance quark-gluon interaction begins to form hadrons. In this respect, the correlation function can be understood by the sum of contributions from all possible intermediate states with appropriate subtractions. The dispersion relation of invariant amplitudes in variable $p_1^2 > 0$ reads

$$F_{ij}(q^2, p_1^2) = \frac{1}{\pi} \int_{m_c^2}^\infty ds\, \frac{{\rm Im}\, F_{ij}(q^2, s)}{s - p_1^2}. \tag{11}$$

By inserting a complete set of hadronic states with the quantum number of the $\bar{c}\gamma_a s$ current, the spectral function of the ground state is obtained from the optical theorem and written by means of two detached matrix elements

$$\epsilon^*_{1a,i'}\rho^0_{ij}(q^2) = \bar{\epsilon}^\mu_i \langle \phi | J^W_{\mu,j}(x) | D^*_s \rangle \langle D^*_s | J^V_a(0) | 0 \rangle, \qquad (12)$$

in which the latter one is parametrized by the D^*_s decay constant, and the former one is written in terms of the $D^*_s \to \phi$ transition form factors associated with orthogonal Lorentz structures [25,26].

$$
\begin{aligned}
&\langle \phi(p_2, \epsilon^*_2) | \bar{s}\gamma_\mu(1-\gamma_5)c | D^*_s(\epsilon_1, p_1) \rangle \\
&= (\epsilon_1 \cdot \epsilon^*_2) \left[p_{1\mu}\mathcal{V}_1(q^2) - p_{2\mu}\mathcal{V}_2(q^2) \right] \\
&\quad + \frac{(\epsilon_1 \cdot q)(\epsilon^*_2 \cdot q)}{m^2_{D^*_s} - m^2_\phi} \left[p_{1\mu}\mathcal{V}_3(q^2) + p_{2\mu}\mathcal{V}_4(q^2) \right] \\
&\quad - (\epsilon_1 \cdot q)\epsilon^*_{2\mu}\mathcal{V}_5(q^2) + (\epsilon_2 \cdot q)\epsilon^*_{1\mu}\mathcal{V}_6(q^2) \\
&\quad - i\varepsilon_{\mu\nu\rho\sigma}\epsilon^\rho_1\epsilon^{*\sigma}_2 \left[p^\nu_1\mathcal{A}_1(q^2) + p^\nu_2\mathcal{A}_2(q^2) \right] \\
&\quad + \frac{i\varepsilon_{\mu\nu\rho\sigma}p^\rho_1 p^\sigma_2}{m^2_{D^*_s} - m^2_\phi} \left[\epsilon^\nu_1(\epsilon^*_2 \cdot q)\mathcal{A}_3(q^2) - \epsilon^\nu_2(\epsilon^*_1 \cdot q)\mathcal{A}_4(q^2) \right],
\end{aligned}
\qquad (13)
$$

here the form factors $\mathcal{V}_j$ and $\mathcal{A}_j$ come from the vector and axial-vector currents, respectively.

We introduce the helicity form factors

$$H_{ij} \equiv \bar{\epsilon}^\mu_i \langle \phi | J^W_{\mu,j} | D^*_s \rangle \qquad (14)$$

and write down the helicity invariant amplitudes as

$$F_{ij}(q^2, p^2_1) = \frac{m_{D^*_s} f_{D^*_s} H_{ij}}{m^2_{D^*_s} - p^2_1} + \int^\infty_{s_0} ds \frac{\rho'^h_{ij}(q^2, s)}{s - p^2_1}. \qquad (15)$$

The relations between helicity form factors and Lorentz orthogonal form factors are collected as

$$
\begin{aligned}
&H_{00}(q^2 > 0) \\
&= \frac{(m^2_{D^*_s} + m^2_\phi - q^2)\lambda^{1/2} \left[-\mathcal{V}_1(q^2) + \mathcal{V}_2(q^2) \right]}{4\sqrt{q^2}m_\phi m_{D^*_s}} \\
&\quad - \frac{\lambda^{1/2} \left[(m^2_{D^*_s} - m^2_\phi - q^2)\mathcal{V}_5(q^2) - (m^2_{D^*_s} - m^2_\phi + q^2)\mathcal{V}_6(q^2) \right]}{4\sqrt{q^2}m_\phi m_{D^*_s}} \\
&\quad + \frac{\lambda^{3/2} \left[\mathcal{V}_3(q^2) + \mathcal{V}_4(q^2) \right]}{8\sqrt{q^2}m_\phi m_{D^*_s}(m^2_{D^*_s} - m^2_\phi)},
\end{aligned}
\qquad (16)
$$

$$
\begin{aligned}
&H_{0\pm}(q^2 > 0) \\
&= -\frac{\lambda^{1/2} \left[\mathcal{V}_1(q^2) - \mathcal{V}_2(q^2) \right]}{2\sqrt{q^2}} \\
&\quad \mp \frac{\left[(m^2_{D^*_s} - m^2_\phi + q^2)\mathcal{A}_1(q^2) + (m^2_{D^*_s} - m^2_\phi - q^2)\mathcal{A}_2(q^2) \right]}{2\sqrt{q^2}},
\end{aligned}
\qquad (17)
$$

$$H_{\pm 0}(q^2 > 0)$$

$$
\begin{aligned}
&= \frac{\lambda^{1/2}\mathcal{V}_6(q^2)}{2m_\phi} \pm \frac{\lambda\mathcal{A}_3(q^2)}{4m_\phi(m^2_{D^*_s} - m^2_\phi)} \\
&\quad \pm \left[\frac{(m^2_{D^*_s} + m^2_\phi - q^2)\mathcal{A}_1(q^2)}{2m_\phi} + m_\phi\mathcal{A}_2(q^2) \right],
\end{aligned}
\qquad (18)
$$

$$H_{\mp\pm}(q^2 > 0)$$

$$
\begin{aligned}
&= \frac{\lambda^{1/2}\mathcal{V}_5(q^2)}{2m_{D^*_s}} \mp \frac{\lambda\mathcal{A}_4(q^2)}{4m_{D^*_s}(m^2_{D^*_s} - m^2_\phi)} \\
&\quad \mp \left[m_{D^*_s}\mathcal{A}_1(q^2) + \frac{(m^2_{D^*_s} + m^2_\phi - q^2)\mathcal{A}_2(q^2)}{2m_{D^*_s}} \right].
\end{aligned}
\qquad (19)
$$

Equations (16–19) show explicitly the kinematical behaviour of the helicity form factors, especially at the end-point $q^2_0 = (m_{D^*_s} - m_\phi)^2$

$$H_{00}(q^2_0) = 0, \quad -H_{0\pm}(q^2_0) = H_{\pm 0}(q^2_0) = H_{\pm\mp}(q^2_0). \quad (20)$$

The endpoint relations as shown in Eq. (20) could be understood in terms of rotational symmetry, reduction of invariant and the Wigner–Eckart theorem [27–29], here we take the last one to explain the relations. According to the Wigner–Eckart theorem, the helicity information in helicity amplitude is only governed by the Clebsch-Gordan (CG) coefficients, and the helicity independent dynamics information is absorbed into the matrix elements M. In our case of $D^*_s(\lambda_{cs}) \to \phi(\lambda_\phi)[l\nu_l](\lambda_q)$ decays, the CG expansion reads as

$$H_{\lambda_q\bar{\lambda}_\phi} = C^{111}_{\lambda_{cs}\lambda_q\bar{\lambda}_\phi}M_{111}. \qquad (21)$$

The helicity conservation equation $\lambda_{cs} = \lambda_q + \bar{\lambda}_\phi$ with $\bar{\lambda}_\phi = -\lambda_\phi$ is self-evident. With taking the CG coefficients $C^{j_{cs}j_\phi j_q}_{\lambda_{cs}\lambda_\phi\lambda_q}$ in the particle data group [1], we obtain

$$
\begin{aligned}
&H_{00}(q^2_0) \propto C^{111}_{000} = 0, \\
&H_{01}(q^2_0) : H_{0\bar{1}}(q^2_0) \propto C^{111}_{101} : C^{111}_{\bar{1}0\bar{1}} = -\frac{1}{2} : \frac{1}{2}, \\
&H_{10}(q^2_0) : H_{\bar{1}0}(q^2_0) \propto C^{111}_{110} : C^{111}_{\bar{1}\bar{1}0} = \frac{1}{2} : -\frac{1}{2}, \\
&H_{\bar{1}1}(q^2_0) : H_{1\bar{1}}(q^2_0) \propto C^{111}_{0\bar{1}1} : C^{111}_{01\bar{1}} = -\frac{1}{2} : \frac{1}{2},
\end{aligned}
\qquad (22)
$$

which reproduce the end-point relations shown in Eq.(20) if we consider the replacement $1(\bar{1}) \leftrightarrow +(-)$ between the helicity quantum numbers and the polarization directions.

Based on the quark-hadron duality, Eqs. (7) and (15) describe the same correlation function from two parallel views, so in principle we can solve the helicity form factors by matching the two equations if we know the spectral functions $\rho'^h_{ij}(s)$. We take the semi-local duality to offset the contributions from large $s > s_0$ regions in the two dispersion relation integrals, because the magnitude of timelike form factor is close to the spacelike one when the momentum transfer is far away from the resonant state regions, and they become equal in the QCD limit [30–32]. We Borel-transform both sides

of the residual contributions below s_0 to suppress the pollutions from excited resonant states and continuum spectral, and arrive at the sum rules of the helicity form factors,

$$
\begin{aligned}
&m_{D_s^*} f_{D_s^*} H_{ij}(q^2) \\
&= \frac{1}{\pi} \int_{m_c^2}^{s_0} ds \frac{e^{-(s+m_{D_s^*}^2)/M^2}}{[u^2(s)m_\phi^2 - q^2 + m_c^2]} \Bigg[u(s) \operatorname{Im} F_{1,ij}^{\mathrm{OPE}}(q^2, s) \\
&\quad + \frac{\operatorname{Im} F_{2,ij}^{\mathrm{OPE}}(q^2, s)}{M^2} + \frac{\operatorname{Im} F_{3,ij}^{\mathrm{OPE}}(q^2, s)}{2u(s)M^4} \Bigg] \\
&\quad + \frac{1}{\pi} \frac{e^{-s_0/M^2}}{[u_0^2 m_\phi^2 - q^2 + m_c^2]} \Bigg[\frac{u_0 \operatorname{Im} F_{2,ij}^{\mathrm{OPE}}(q^2, s_0)}{s_0 - q^2} \\
&\quad + \frac{(1+x_{s_0})\operatorname{Im} F_{3,ij}^{\mathrm{OPE}}(q^2, s_0) - u_0 \operatorname{Im} F_{3,ij}^{\prime\mathrm{OPE}}(q^2, s_0)}{2(s_0 - q^2)^2} \Bigg].
\end{aligned}
$$
(23)

Here u_0 is the solution of $s_0 = \bar{u}m_\phi^2 + (m_c^2 - \bar{u}q^2)/u$, $x_{s_0} \equiv (s_0-q^2)/M^2$ and $\operatorname{Im} F_{3,ij}^{\prime\mathrm{OPE}}(q^2, s_0) = \frac{\partial}{\partial s}\operatorname{Im} F_{3,ij}^{\mathrm{OPE}}(q^2, s)|_{s=s_0}$.

The value of Borel mass squared is implied by the internal virtuality of propagator which is smaller than the cutoff threshold value, saying $M^2 \sim \mathcal{O}(um_{D_s^*}^2 + \bar{u}Q^2 - u\bar{u}m_\phi^2) < s_0$, this value is a litter bit larger than the factorisation scale we chosen at $\mu_f^2 = m_{D_s^*}^2 - m_c^2 = 1.66^2\,\mathrm{GeV}^2$ with the quark mass $\overline{m}_c(m_c) = 1.30\,\mathrm{GeV}$. In practice the selection of Borel mass is actually a compromise between the overwhelming chosen of ground state in hadron spectral that demands a small value and the convergence of OPE evaluation that prefers a large one, which result in a region where $H_{ij}(q^2)$ shows an extremum in M^2 [24,25]

$$
\frac{d}{d(1/M^2)} \ln H_{ij}(q^2) = 0.
$$
(24)

The continuum threshold is usually set to close to the outset of the first excited state with the same quantum number as D_s^* and characterised by $s_0 \approx (m_{D_s^*} + \chi)^2$, which is finally determined by considering the maximal stable evolution of physical quantities on the Borel mass squared. From the numerical side, the chose of these two parameters should guaratee the convergence of twist expansion in the truncated OPE calculation (high twists contributions are no more than thirty percents) and simultaneously the high energy cutoff in the hadron interpolating (the contributions from high excited state and continuum spectral is smaller than thirty percents). We finally set them at $M^2 = 4.5 \pm 1.0\,\mathrm{GeV}^2$ and $s_0 = 6.8 \pm 1.0\,\mathrm{GeV}^2$ in this work. The value of Borel mass is a litter bit larger than it chosen in the $D_s \to \pi, K$ transition [13], while a litter bit smaller than it chosen in the $D_s \to \phi, f_0(980)$ transition [16], and close to it chosen in the $D_s \to \eta'$ transition [15].

The tree level LCSRs prediction of modified helicity form factors $\mathcal{H}_{ij}(q^2) \equiv \sqrt{q^2} H_{ij}(q^2)$ are depicted in Fig. 1 where the uncertainties from the Borel mass and the continuum

Table 1 The anatomy of the LCSRs uncertainty of helicity form factors $\mathcal{H}_{ij}(q^2)$, the center value (CV) is obtained by setting $M^2 = 4.5\,\mathrm{GeV}^2$ and $s_0 = 6.8\,\mathrm{GeV}^2$

$\mathcal{H}_{ij}(q^2)$	CV	$M^2\vert_{-1.0}^{+1.0}$	$s_0\vert_{-1.0}^{+1.0}$
$\mathcal{H}_{00}(0.04)$	1.99	-0.07 $+0.13$	$+0.09$ -0.15
$\mathcal{H}_{00}(0.20)$	2.03	-0.09 $+0.16$	$+0.09$ -0.16
$\mathcal{H}_{00}(0.40)$	2.07	-0.11 $+0.20$	$+0.09$ -0.16
$\mathcal{H}_{0+}(0.04)$	2.85	$+0.05$ -0.08	$+0.21$ -0.33
$\mathcal{H}_{0+}(0.20)$	2.82	$+0.05$ -0.07	$+0.21$ -0.34
$\mathcal{H}_{0+}(0.40)$	2.78	$+0.04$ -0.07	$+0.22$ -0.35
$\mathcal{H}_{0-}(0.04)$	0.19	$+0.03$ -0.05	$+0.05$ -0.08
$\mathcal{H}_{0-}(0.20)$	0.18	$+0.04$ -0.06	$+0.06$ -0.09
$\mathcal{H}_{0-}(0.40)$	0.17	$+0.04$ -0.07	$+0.07$ -0.11
$\mathcal{H}_{+0}(0.04)$	0.53	-0.05 $+0.09$	$+0.01$ -0.02
$\mathcal{H}_{+0}(0.20)$	1.07	-0.11 $+0.21$	$+0.02$ -0.04
$\mathcal{H}_{+0}(0.40)$	1.61	-0.16 $+0.31$	$+0.03$ -0.05
$\mathcal{H}_{-0}(0.04)$	-0.59	$+0.05$ -0.10	-0.03 $+0.04$
$\mathcal{H}_{-0}(0.20)$	-1.36	$+0.13$ -0.24	-0.07 $+0.08$
$\mathcal{H}_{-0}(0.40)$	-2.00	$+0.20$ -0.38	-0.09 $+0.11$
$\mathcal{H}_{+-}(0.04)$	0.42	$+0.01$ -0.01	$+0.03$ -0.05
$\mathcal{H}_{+-}(0.20)$	0.94	$+0.01$ -0.01	$+0.08$ -0.12
$\mathcal{H}_{+-}(0.40)$	1.31	$+0.01$ -0.01	$+0.11$ -0.17
$\mathcal{H}_{-+}(0.04)$	-0.04	-0.01 $+0.02$	-0.01 $+0.01$
$\mathcal{H}_{-+}(0.20)$	-0.07	-0.02 $+0.03$	-0.01 $+0.02$
$\mathcal{H}_{-+}(0.40)$	-0.09	-0.02 $+0.04$	-0.02 $+0.03$

threshold are presented by iteration. The Borel mass dependence of these modified helicity form factors are plotted in Fig. 2. The anatomy of the LCSRs uncertainty are presented in Table 1 by taking the result at three momentum transfer points, saying $q^2 = 0.04, 0.20$ and $0.40\,\mathrm{GeV}^2$. It shows that

(1) Our choice of Borel mass brings 5–10% uncertainty to the helicity form factor $\mathcal{H}_{00}$, 10–20% uncertainty to $\mathcal{H}_{+0}$ and $\mathcal{H}_{-0}$, 20–30% uncertainty to $\mathcal{H}_{0-}$ and $\mathcal{H}_{-+}$, and less than 5% uncertainty to $\mathcal{H}_{0+}$, it almost does not bring uncertainty to the helicity form factor $\mathcal{H}_{+-}$.

(2) Our choice of continuum threshold brings another 5%–10% uncertainty to the helicity form factor $\mathcal{H}_{00}$, 10% uncertainty to $\mathcal{H}_{0+}$ and $\mathcal{H}_{+-}$, 20–30% uncertainty to $\mathcal{H}_{-+}$, and 30–40% uncertainty to $\mathcal{H}_{0-}$, it does not bring additional uncertainty to the helicity form factors $\mathcal{H}_{+0}$ and $\mathcal{H}_{-0}$.

(3) The LCSRs uncertainty of form factors $\mathcal{H}_{00}$, $\mathcal{H}_{\pm 0}$ and $\mathcal{H}_{-+}$ mainly comes from the Borel mass, the LCSRs uncertainty of $\mathcal{H}_{0-}$ comes equivalently from Borel mass and continuum threshold, meanwhile it in form factors

Fig. 1 The LCSRs predictions of modified helicity form factors $\mathcal{H}_{ij}(q^2) \equiv \sqrt{q^2} H_{ij}(q^2)$ with varying Borel mass in $4.5 \pm 1.0\,\text{GeV}^2$ and fixing continuum threshold at $s_0 = 6.8\,\text{GeV}^2$ (Gray), with varying Borel mass in $4.5 \pm 1.0\,\text{GeV}^2$ and continuum threshold in $s_0 = 6.8 \pm 1.0\,\text{GeV}^2$ (LightGray)
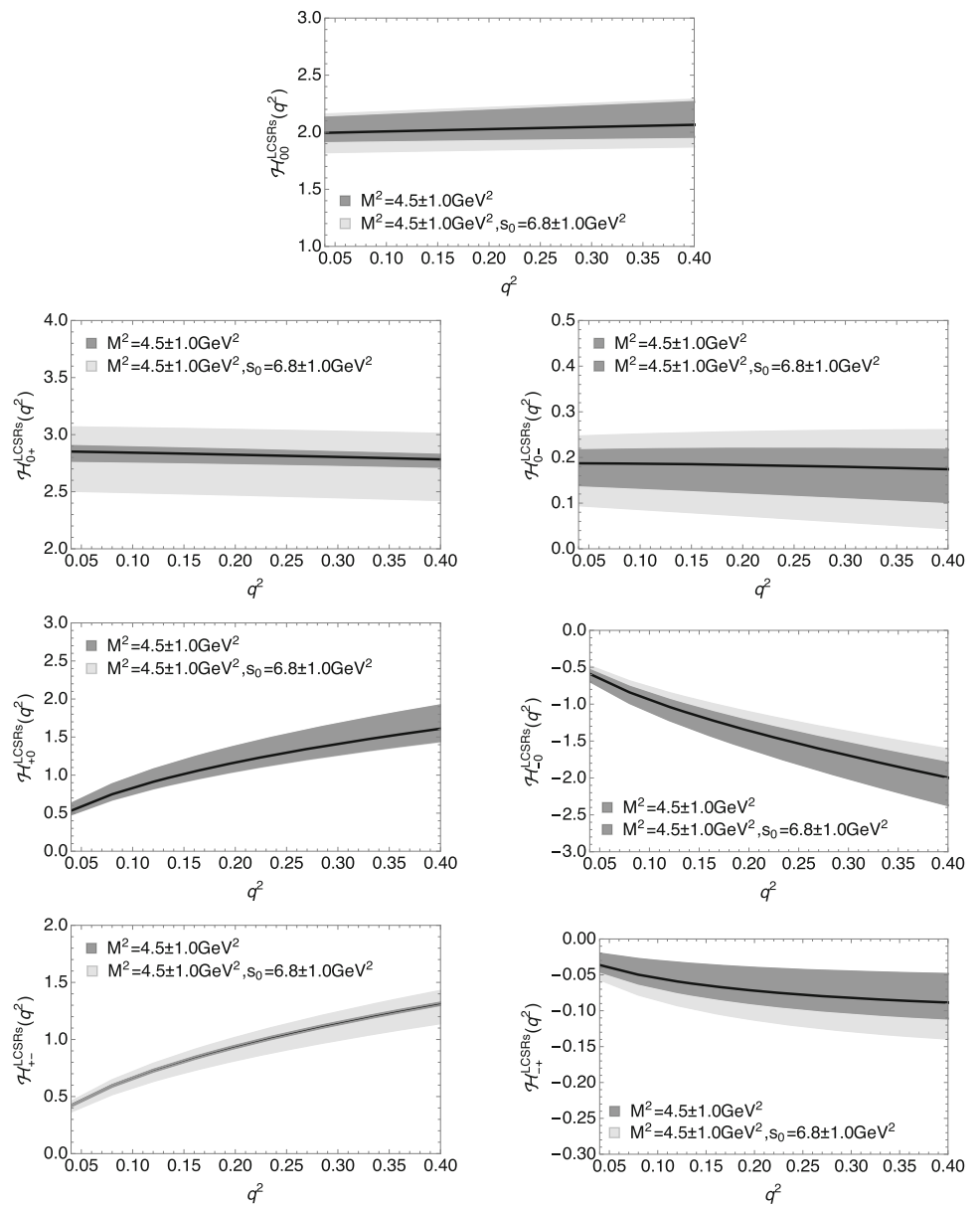
$\mathcal{H}_{0+}$ and $\mathcal{H}_{+-}$ mainly arises from the continuum threshold.

(4) These modified helicity form factors have different monotonicities on the two LCSRs parameters, for example, $\mathcal{H}_{0\pm}$, $\mathcal{H}_{-0}$ and $\mathcal{H}_{+-}$ are monotonically increasing on M^2, others are monotonically decreasing on M^2, as shown in Fig. 2 where the Borel mass dependence of these seven helicity form factors are presented at three different momentum transfer points $q^2 = 0.04, 0.20$ and $0.40\,\text{GeV}^2$. The magnitudes of all seven modified helicity form factors are all monotonically increasing on the continuum threshold.

In Table 2, we show the LCSRs prediction of modified helicity form factors at the fixed momentum transfer points, saying from 0.04 to 0.4 GeV with the step 0.04 GeV. The

first uncertainties come from the LCSRs parameters M^2 and s_0 which is added by the quadratic sum. In order to estimate the effect from the missing radiative corrections, we vary the charm quark mass in the interval $\overline{m}_c(m_c) = 1.30 \pm 0.10\,\text{GeV}$ and regard this possible NLO effect as the second uncertainty. The facotrization scale is then varied in $\mu_f = 1.66 \pm 0.08\,\text{GeV}$ correspondingly. It brings about 10% additional uncertainty to the modified helicity form factors $\mathcal{H}_{\pm 0}$ and $\mathcal{H}_{-+}$, 15% additional uncertainty to $\mathcal{H}_{00}$ and $\mathcal{H}_{0+}$, 20% additional uncertainty to $\mathcal{H}_{+-}$, meanwhile 40% additional uncertainty to $\mathcal{H}_{0-}$. We examined the affect to the Borel mass determination from the quark mass variation and found that $M^2 = 4.5 \pm 1.0\,\text{GeV}^2$ is still the optimal choice. We do not present the uncertainty from the nonperturbative parameters in ϕ meson LCDAs as shown in Table 4, since the decay constants from the lattice evaluation almost do not

Fig. 2 The Borel mass dependence of all seven modified helicity form factors in our considering where the continuum threshold is set at 6.8 GeV^2. Three curves at different momentum transfer points are shown for each form factor
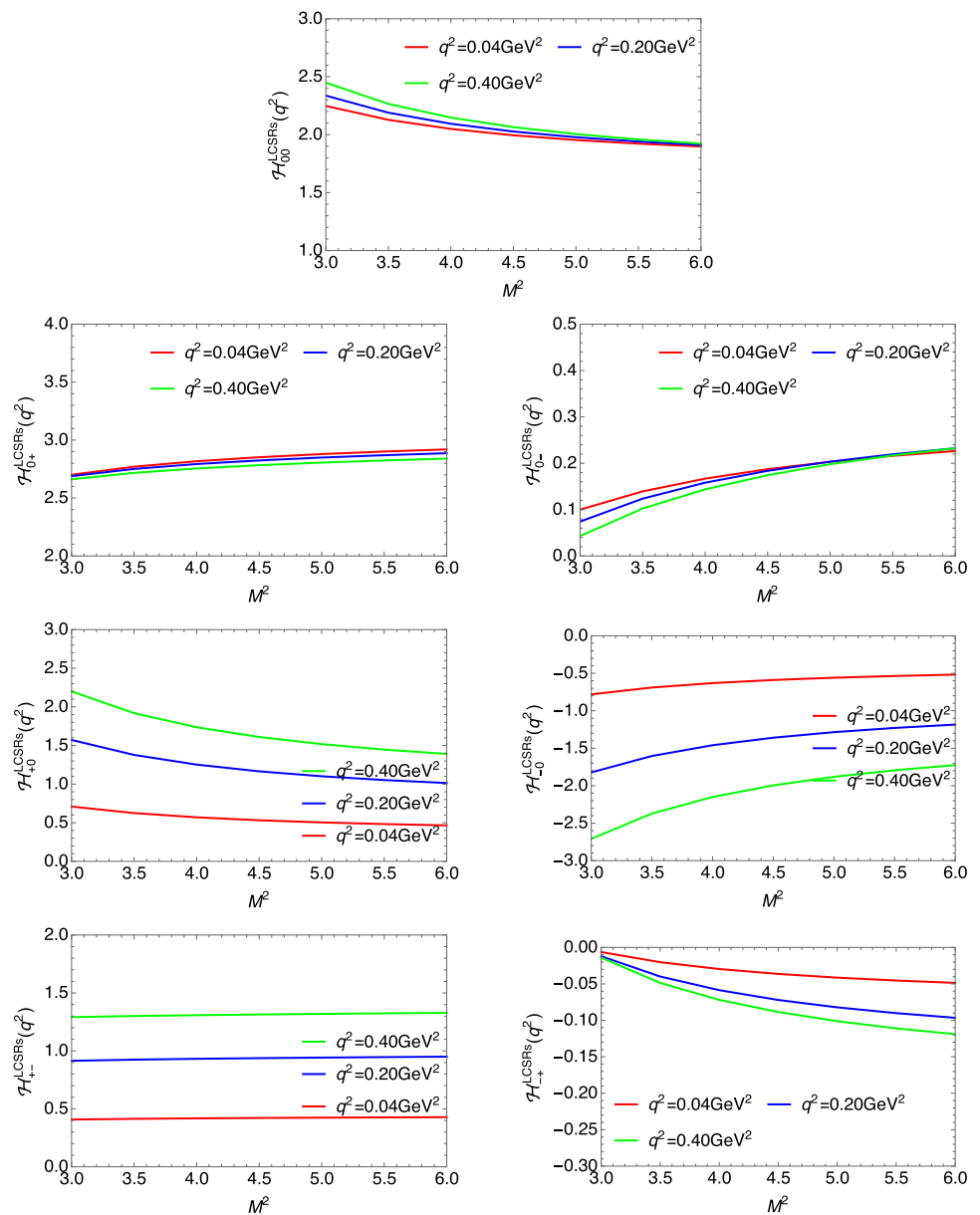

Table 2 The modified helicity form factor $\mathcal{H}_{ij}(q^2) \equiv \sqrt{q^2} H_{ij}(q^2)$ in the large recoiled regions from LCSRs

q^2(GeV^2)	$\mathcal{H}_{00}(q^2)$	$\mathcal{H}_{0+}(q^2)$	$\mathcal{H}_{0-}(q^2)$	$\mathcal{H}_{+0}(q^2)$	$\mathcal{H}_{-0}(q^2)$	$\mathcal{H}_{+-}(q^2)$	$\mathcal{H}_{-+}(q^2)$
0.04	$1.99^{+0.16+0.32}_{-0.17-0.29}$	$2.85^{+0.21+0.48}_{-0.35-0.47}$	$0.19^{+0.06+0.09}_{-0.09-0.07}$	$0.53^{+0.09+0.06}_{-0.05-0.06}$	$-0.59^{-0.11-0.07}_{+0.07+0.07}$	$0.42^{+0.03+0.08}_{-0.05-0.07}$	$-0.04^{-0.01-0.00}_{+0.02+0.00}$
0.08	$2.00^{+0.17+0.31}_{-0.17-0.29}$	$2.85^{+0.21+0.48}_{-0.35-0.47}$	$0.19^{+0.06+0.09}_{-0.10-0.07}$	$0.75^{+0.13+0.08}_{-0.07-0.08}$	$-0.84^{-0.15-0.10}_{+0.10+0.10}$	$0.60^{+0.05+0.11}_{-0.08-0.10}$	$-0.05^{-0.02-0.00}_{+0.03+0.01}$
0.12	$2.01^{+0.17+0.31}_{-0.18-0.29}$	$2.84^{+0.22+0.47}_{-0.35-0.46}$	$0.19^{+0.07+0.08}_{-0.10-0.07}$	$0.91^{+0.16+0.10}_{-0.09-0.10}$	$-1.04^{-0.19-0.12}_{+0.12+0.12}$	$0.73^{+0.06+0.14}_{-0.09-0.13}$	$-0.06^{-0.02-0.01}_{+0.03+0.01}$
0.16	$2.02^{+0.18+0.30}_{-0.18-0.29}$	$2.83^{+0.22+0.47}_{-0.35-0.46}$	$0.18^{+0.07+0.08}_{-0.11-0.07}$	$1.05^{+0.19+0.11}_{-0.11-0.11}$	$-1.21^{-0.22-0.14}_{+0.14+0.13}$	$0.84^{+0.07+0.16}_{-0.11-0.15}$	$-0.07^{-0.02-0.01}_{+0.04+0.01}$
0.20	$2.03^{+0.19+0.30}_{-0.18-0.28}$	$2.82^{+0.22+0.46}_{-0.35-0.46}$	$0.18^{+0.07+0.08}_{-0.11-0.07}$	$1.07^{+0.21+0.12}_{-0.12-0.12}$	$-1.36^{-0.25-0.15}_{+0.15+0.15}$	$0.94^{+0.08+0.17}_{-0.12-0.16}$	$-0.07^{-0.02-0.01}_{+0.04+0.01}$
0.24	$2.03^{+0.19+0.29}_{-0.18-0.28}$	$2.82^{+0.22+0.46}_{-0.35-0.45}$	$0.18^{+0.08+0.08}_{-0.11-0.07}$	$1.27^{+0.23+0.13}_{-0.13-0.13}$	$-1.50^{-0.28-0.17}_{+0.17+0.16}$	$1.03^{+0.09+0.19}_{-0.13-0.18}$	$-0.08^{-0.02-0.01}_{+0.04+0.01}$
0.28	$2.04^{+0.20+0.29}_{-0.18-0.28}$	$2.81^{+0.22+0.45}_{-0.35-0.45}$	$0.18^{+0.08+0.08}_{-0.11-0.07}$	$1.37^{+0.25+0.14}_{-0.14-0.14}$	$-1.63^{-0.31-0.18}_{+0.19+0.17}$	$1.11^{+0.09+0.20}_{-0.14-0.19}$	$-0.08^{-0.03-0.01}_{+0.05+0.01}$
0.32	$2.05^{+0.21+0.29}_{-0.19-0.27}$	$2.80^{+0.22+0.45}_{-0.35-0.45}$	$0.18^{+0.08+0.08}_{-0.12-0.07}$	$1.45^{+0.27+0.14}_{-0.15-0.15}$	$-1.76^{-0.34-0.19}_{+0.20+0.19}$	$1.18^{+0.10+0.22}_{-0.15-0.20}$	$-0.08^{-0.03-0.01}_{+0.05+0.01}$
0.36	$2.06^{+0.21+0.28}_{-0.19-0.27}$	$2.79^{+0.22+0.45}_{-0.36-0.44}$	$0.18^{+0.08+0.08}_{-0.12-0.07}$	$1.53^{+0.29+0.15}_{-0.16-0.15}$	$-1.88^{-0.36-0.21}_{+0.21+0.20}$	$1.25^{+0.11+0.23}_{-0.16-0.21}$	$-0.09^{-0.03-0.01}_{+0.05+0.01}$
0.40	$2.07^{+0.22+0.28}_{-0.19-0.27}$	$2.78^{+0.22+0.44}_{-0.36-0.44}$	$0.17^{+0.09+0.08}_{-0.12-0.07}$	$1.61^{+0.31+0.15}_{-0.17-0.16}$	$-2.00^{-0.39-0.22}_{+0.23+0.21}$	$1.31^{+0.11+0.24}_{-0.17-0.22}$	$-0.09^{-0.03-0.01}_{+0.05+0.01}$

bring additional uncertainty and the the uncertainty associated to strange quark mass is less than two percent.

We remark again that the main target of this work is to discuss a feasible measurement of the weak decay of vector meson, so the staring point for the calculation is the multiplied correlation function in Eq. (5) which deduces to the helicity form factors. Moreover, what we have indeed calculated is the seven helicity form factors involved in the semileptonic weak decay, and hence we can not obtain the ten orthogonal Lorentz form factors corresponding to the correlation function in Eq. (2) by a linearly variation. But their relations as shown in Eqs. (16–19) provide some constraints to deduce the orthogonal Lorentz form factors. For example, the (modified) helicity form factors at the full recoiled point $q^2 = 0$ are

$$
\begin{aligned}
&\mathcal{H}_{00}(0) = 1.99^{+0.15+0.32}_{-0.17-0.30}, \\
&\mathcal{H}_{0+}(0) = 2.86^{+0.21+0.48}_{-0.35-0.48}, \quad \mathcal{H}_{0-}(0) = 0.19^{+0.05+0.09}_{-0.09-0.07}, \\
&H_{+0}(0) = 2.67^{+0.47+0.31}_{-0.26-0.29}, \quad H_{-0}(0) = -2.92^{-0.53-0.35}_{+0.33+0.32}, \\
&H_{+-}(0) = 2.11^{+0.17+0.40}_{-0.27-0.28}, \quad H_{-+}(0) = -0.19^{-0.06-0.01}_{+0.11+0.03},
\end{aligned}
\tag{25}
$$

from which we can deduce the center values of several orthogonal Lorentz form factors as $\mathcal{V}_1(0) - \mathcal{V}_2(0) = -1.86$, $\mathcal{V}_5(0) = 2.46$, $\mathcal{V}_6(0) = -0.26$, and $\mathcal{A}_1(0) + \mathcal{A}_2(0) = -1.63$. These value can be compared with the result obtained from other approaches such as the light-front quark model [26], and in fact they show a good consistence after considering the different definitions of $\mathcal{V}_{i=1-6}$ and $\mathcal{A}_{i=1-4}$ in Eq. (13) here and Eqs. (2.1, 2.2) there.

To extrapolate to the whole kinematic region $[0, q_0^2]$, we adopt the SSE parameterisation [19] which is required not only to reproduce the result obtained from LCSRs calculation in the lower interval $[0, q^2_{\mathrm{LCSR,max}}]$ with good accuracy, but also to provide an extrapolation to the up interval $[q^2_{\mathrm{LCSR,max}}, q_0^2]$ with the expected analytical properties of the helicity form factors. For the maximal momentum transfer squared where LCSRs is still applicable, we take it at $m_c^2 - 2m_c\chi \sim 0.4\,\mathrm{GeV}^2$ with $\chi \sim 0.5\,\mathrm{GeV}$ being a typical hadronic scale, as what have been done in $D_{(s)}$ decays [13,14]. We truncate the simplified z-series expansion after the linear term for the Lorentz orthogonal form factors $\mathcal{F}_i = \mathcal{V}_{1-6}, \mathcal{A}_{1-4}$,

$$
\mathcal{F}_i(q^2 > 0) = \frac{a_{\mathcal{F}_i}}{1 - q^2/m_{D1}^2}\left\{1 + b_{\mathcal{F}_i}\left[z(q^2) - z(0)\right]\right\},
\tag{26}
$$

the quadratic term is checked could be negligible here. In the expansion, $1/(1 - q^2/m_{D1}^2)$ denotes the simple pole corresponding to the lowest-lying resonance in the $D_s^*\phi$ spectrum with $m_{D1} = 2.77\,\mathrm{GeV}$ [1], $a_{\mathcal{F}_i} \equiv \mathcal{F}_i(0)$ indicates the normalization conditions. The SSE formula bases on a rapidly

converging series

$$
z(q^2) = \frac{\sqrt{t_+ - q^2} - \sqrt{t_+ - t_0}}{\sqrt{t_+ - q^2} + \sqrt{t_+ - t_0}}
\tag{27}
$$

with $t_\pm \equiv (m_{D_s^*} \pm m_\phi)^2$ and $t_0 \equiv t_+(1 - \sqrt{1 - t_-/t_+})$.

We parameterize the helicity form factors by considering their general kinematical behavious in Eqs. (16–19) and their end-point relations in Eq. (20), their expressions are

$$
\begin{aligned}
\mathcal{H}_{ij}^{\mathrm{SSE}}(q^2) &\equiv \sqrt{q^2}H_{ij}(q^2) \\
&= \mathcal{K}_{ij}(q^2)\frac{1 + b_{ij}z'(q^2)}{(1 - q^2/m_{D1}^2)}\Bigg[\frac{a_{ij}^1 \lambda^{3/2}}{m_{D_s^*}m_\phi(m_{D_s^*}^2 - m_\phi^2)} \\
&\quad + \frac{a_{ij}^2 \lambda}{(m_{D_s^*}^2 - m_\phi^2)} + a_{ij}^3 \lambda^{1/2}\Bigg] \\
&\quad + \kappa_{ij}q_0\Bigg[m_{D_s^*}\frac{1 + b_1^{\mathbf{ED}}z'(q^2)}{(1 - q^2/m_{D1}^2)} + m_\phi\frac{1 + b_2^{\mathbf{ED}}z'(q^2)}{(1 - q^2/m_{D1}^2)}\Bigg].
\end{aligned}
\tag{28}
$$

Here $z'(q^2) \equiv z(q^2) - z(0)$ and $q_1^2 \equiv q_0^2 - q^2$. The kinematical functions/factors read as

$$
\begin{aligned}
&\mathcal{K}_{00}(q^2) = \frac{\lambda^{1/2}}{m_{D_s^*}m_\phi}, \quad \kappa_{00} = 0; \\
&\mathcal{K}_{ij\neq00} = 1; \quad \kappa_{0\mp}(q^2) = \kappa_{\pm0}(q^2) = \kappa_{\pm\mp}(q^2) = \pm1; \\
&a_{0\pm}^1 = a_{\pm0}^1 = a_{\pm\mp}^1 = 0, \quad a_{0\pm}^2 = 0.
\end{aligned}
\tag{29}
$$

We can see that the terms in the third line on the right hand side give the result of form factors $\mathcal{H}_{ij\neq00}$ at the kinematical end-point with the universal parameters $b_{1,2}^{\mathbf{ED}}$, and the general terms in the first two lines hint the end-point constraint of $\mathcal{H}_{00}(q_0^2) = 0$.

With setting $q^2_{\mathrm{LCSR,max}} = 0.4\,\mathrm{GeV}^2$, the fit result of SSE parameters are shown in Table 3. We mark that the superscript and subscript numbers are not the errors, but the differences to the central value fitted by the upper and lower predictions of the helicity form factors from LCSRs, respectively. We depict the modified helicity form factors in Fig. 2, where the result obtained directly from LCSRs calculation is shown by lightblue bands, and the extrapolation by z-series parameterisation is shown by red bands. The form factors at end-point are obtained as $\mathcal{H}_{00}^{\mathrm{SSE}}(q_0^2) = 0$ and $|\mathcal{H}_{ij\neq00}^{\mathrm{SSE}}(q_0^2)| = 0.23^{+0.18}_{-0.23}$. The end-point constraints play an important role to set down the shapes of helicity form factors in the small recoiled regions where the LCSRs calculation is failed, in coordination with the kinematical structures in Eqs. (16–19). Besides the SSE parameterisation of the form factors, we have also tested the Becirevic and Kaidalov (BK) parameterisation [20] and found almost the same fit result of the helicity form factors.

Table 3 The SSE parameters of the helicity form factors $\mathcal{H}_{ij}(q^2)$

Para.	$\mathcal{H}_{00}(q^2)$	$\mathcal{H}_{0+}(q^2)$	$\mathcal{H}_{0-}(q^2)$	$\mathcal{H}_{+0}(q^2)$	$\mathcal{H}_{-0}(q^2)$	$\mathcal{H}_{+-}(q^2)$	$\mathcal{H}_{-+}(q^2)$
a^1_{ij}	$0.70^{+0.21}_{-0.05}$	0	0	0	0	0	0
a^2_{ij}	$-2.55^{-0.79}_{+0.58}$	0	0	$-2.00^{-0.76}_{+0.27}$	$3.46^{-2.29}_{+0.60}$	$-1.56^{-0.24}_{+0.24}$	$0.96^{-0.09}_{+0.04}$
a^3_{ij}	$1.81^{+0.52}_{-0.57}$	$1.83^{+0.16}_{-0.16}$	$-0.95^{+0.03}_{-0.03}$	$1.10^{+0.78}_{-0.29}$	$-2.56^{+2.30}_{-0.72}$	$0.64^{+0.26}_{-0.24}$	$0.03^{+0.09}_{-0.04}$
b_{ij}	$-17.48^{-27.5}_{+4.25}$	$2.20^{-2.15}_{+2.75}$	$18.08^{-0.68}_{+0.66}$	$42.18^{+1.31}_{-3.66}$	$23.85^{+26.5}_{-0.78}$	$36.27^{+4.72}_{-5.88}$	$0.08^{-0.17}_{+2.84}$
b^{ED}_1	0		$39.24^{-2.10}_{+1.86}$		$39.24^{-2.10}_{+1.86}$		$39.24^{-2.10}_{+1.86}$
b^{ED}_2	0		$18.85^{-1.13}_{+1.12}$		$18.85^{-1.13}_{+1.12}$		$18.85^{-1.13}_{+1.12}$

Fig. 3 The helicity form factors $\mathcal{H}_{ij}(q^2)$ obtained from the LCSRs calculation in the large recoiled regions and the extrapolating to the whole kinematical region by SSE parameterization
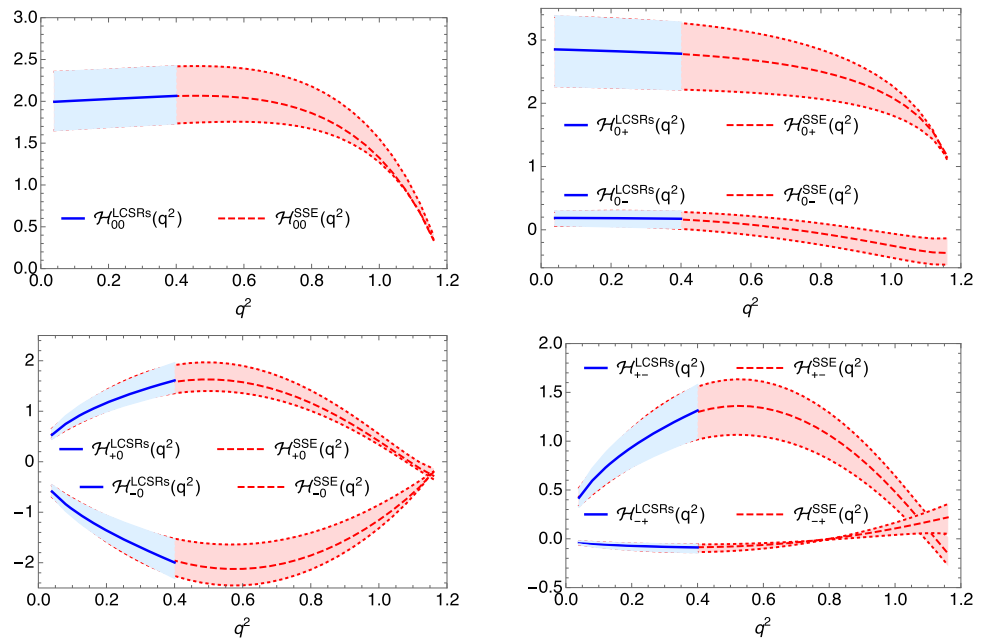
3 Exclusive D_s^* weak decays

The leptonic decays $D_s^* \rightarrow \ell\nu$ ($\ell = e, \mu$) have the decay width

$$\Gamma_{D_s^* \rightarrow l\nu} = \frac{G_F^2}{12\pi}|V_{cs}|^2 f_{D_s^*}^2 m_{D_s^*}^3 = 2.44 \times 10^{-12} \text{ GeV}, \quad (30)$$

if we accept the lattice result of the decay constant $f_{D_s^*} = 0.274$ GeV [9] and neglect the lepton masses. The differential decay width of semileptonic decays of a particular polarization mode is written as

$$\frac{d\Gamma_{ij}}{dq^2} = \frac{G_F^2 |V_{cs}|^2 \lambda^{1/2} q^2}{192\pi^3 m_{D_s^*}^3}|\mathcal{H}_{ij}(q^2)|^2. \quad (31)$$

With the helicity form factors obtained above, we obtain the spin averaged total decay width

$$\Gamma_{D_s^* \rightarrow \phi l \nu_l} = \frac{1}{3}\int_0^{q_0^2} dq^2 \sum_{i,j=0,\pm} \frac{d\Gamma_{ij}}{dq^2}$$
$$= (3.28^{+0.82}_{-0.71}) \times 10^{-14} \text{ GeV}. \quad (32)$$

The leptonic and semileptonic D_s^* weak decays, meanwhile, extent the investigation of lepton flavour university (LFU) study [33–35].

Under the naive factorisation hypothesis with considering only the color singlet operator at tree level, the decay amplitudes of $D_s^* \rightarrow \phi\pi, \phi\rho$ channels are detached into two matrix elements,

$$\mathcal{A}_{D_s^{*+} \rightarrow \phi\pi^+} = (-i)\frac{G_F}{\sqrt{2}}V_{cs}a_1 m_\pi f_\pi \sum_{j=0,\pm} \mathcal{H}_{0j}(m_\pi^2),$$

$$\mathcal{A}_{D_s^{*+} \rightarrow \phi\rho^+} = \frac{G_F}{\sqrt{2}}V_{cs}a_1 m_\rho f_\rho^\| \sum_{i,j=0,\pm} \mathcal{H}_{ij}(m_\rho^2). \quad (33)$$

Considering the wilson coefficient $a_1 = 0.999$ at the factorisation scale $\mu = (m_{D_s^*}^2 - m_c^2)^{1/2}$ [36] and the decay constants $f_\pi = 0.130$ GeV [1] and $f_\rho^\| = 0.210$ GeV [24], we obtain the partial widths of nonleptonic decays as

$$\Gamma_{D_s^{*+} \rightarrow \phi\pi^+} = (3.81^{+1.52}_{-1.33}) \times 10^{-14} \text{ GeV},$$

$$\Gamma_{D_s^{*+} \rightarrow \phi\rho^+} = (1.16^{+0.42}_{-0.39}) \times 10^{-13} \text{ GeV}. \quad (34)$$

The large uncertainty (40%) in $\phi\pi$ channel comes from the LCSRs predictions of the helicity form factors at the momentum transfer point $q^2 = m_\pi^2$, meanwhile the uncertainty ($\sim 40\%$) in $\phi\rho$ channel comes from the extrapolation by simplified z-series expansion at the momentum transfer point $q^2 = m_\rho^2$. The prediction of $\Gamma_{D_s^{*+}\to\phi\pi^+}$ is marginally consistent with the recent calculation based on the perturbative QCD approach [37], but is half smaller in the magnitude. We mark that the color mixing operator (a_2 proportional) at tree level and the non-perturbative contributions are usually significant, and could give sizable contributions to the hadronic decays, accompanying with the contribution from timelike polarisation of leptonic current $\bar{\epsilon}_\mu(t)$. We postpone these contributions for the further study. If we take the total width $\Gamma_{D_s^*} = (7.0 \pm 2.8) \times 10^{-8}$ GeV evaluated from lattice QCD [9], the branching fractions of D_s^* weak decays are

$$\mathcal{B}(D_s^* \to l\nu) = (3.49 \pm 0.14) \times 10^{-5},$$
$$\mathcal{B}(D_s^* \to \phi l\nu) = (0.47^{+0.12}_{-0.10} \pm 0.19) \times 10^{-6},$$
$$\mathcal{B}(D_s^* \to \phi\pi) = (0.54^{+0.22}_{-0.19} \pm 0.22) \times 10^{-6},$$
$$\mathcal{B}(D_s^* \to \phi\rho) = (1.65^{+0.61}_{-0.56} \pm 0.66) \times 10^{-6}. \tag{35}$$

Let us give a brief discussion on the experimental potential of D_s^* weak decays. The integrated luminosity at Belle II would achieve $10\,\text{ab}^{-1}$ after the phase 3 running (2024-2026) [38], which would produce an available $D_s(D_s^*)$ sample at order $\mathcal{O}(10^9)$ by considering $\mathcal{O}(10^6)$ $D_s \to \phi(KK)\pi^+$ signals (with efficiency 22%) are obtained based on $921\,\text{fb}^{-1}$ data sample [39,40] and the branching fraction $B(D_s \to \phi(KK)\pi) = 2.24\%$ [1]. With this sample, about $\mathcal{O}(10^7)$ $(\mathcal{O}(10^2))$ signals of $D_s(D_s^*) \to \phi(KK)\pi$ would be obtained, which indicates the feasibility of searching for $D_s^* \to \phi\pi$ at Belle II. Meanwhile, about 3.07×10^6 D_s^* mesons have been collected by BESIII with the integrated luminosity $3.2\,\text{fb}^{-1}$ at 4.178 GeV [41]. They are directly produced from the e^+e^- collision at the $D_s D_s^*$ threshold with lower background, and it provides a good chance to measure the leptonic decays $D_s^* \to l\nu$ and to further determine $\Gamma_{D_s^*}$. Note that the photon-radiation effect is tiny in the leptonic D_s^* decays since these channels are not helicity suppressed in contrast to the $D_s \to l\nu$ decays. For the hadronic decay channels, we hope LHCb, with the excellent particle identification to distinguish K, π and μ, would study the $D_s^* \to \phi(KK)\pi$ channel with D_s^* producing from semileptonic decay $B_s \to D_s^* \mu\nu$ [42].

4 Summary

In this work we calculate the $D_s^* \to \phi$ helicity form factors from LCSRs with the accuracy up to two-particle twist-5 DAs of the ϕ meson at the leading order of α_s, with which we study the experimental potential of discovering D_s^* weak

decays. The result shows that the leptonic decays $D_s^* \to l\nu$ are the most hopeful channels to be measured at BESIII, the semileptonic decays $D_s^* \to \phi l\nu$ could be accessible at Belle II after the phase 3 running, and the hadronic $D_s^* \to \phi\pi$ decays are promising at LHCb. The measurement of purely leptonic decays would determine the total width of the D_s^* meson and hence clarify some fundamental properties of the D_s^* meson, such as the electromagnetic and strong couplings $g_{D_s^* D_s \gamma}$ and $g_{D_s^* D_s \pi}$. It is highly hopeful that these channels will promote the first observation of weak decays of a vector meson, opening up a new playground to test the standard model and pushing us to higher precision studies.

A Definition of ϕ meson on the light cone

In order to facilitate the light-cone expansion, the meson four-momentum (p_μ) and close to lightlike separation (x_μ) are expressed as linear combinations of the lightlike vectors ($\hat{p}_\mu, z_\mu$) [32],

$$\hat{p}_\mu = p_\mu - \frac{1}{2} z_\mu \frac{m_M^2}{\hat{p} \cdot z},$$
$$z_\mu = x_\mu \left[1 - \frac{x^2 m_M^2}{4(\hat{p} \cdot z)^2} \right] - \frac{1}{2} \hat{p}_\mu \frac{x^2}{\hat{p} \cdot z} + \mathcal{O}(x^4). \tag{36}$$

Meanwhile, the polarization vectors decompose into three terms,

$$
\epsilon_\mu^\lambda = \frac{\epsilon^\lambda \cdot x}{\hat{p} \cdot z} \hat{p}_\mu + \frac{\epsilon^\lambda \cdot \hat{p}}{\hat{p} \cdot z} z_\mu + \epsilon_{\perp\mu}^\lambda
$$
$$
= (\epsilon^\lambda \cdot x) \frac{p_\mu (p \cdot x) - x_\mu m_M^2}{(p \cdot x)^2 - x^2 m_M^2}. \tag{37}
$$

Here λ is the polarisation of meson and we use the symbols $\parallel$, $\perp$ to denote the longitudinal and transversal directions of the polarizations, respectively.

LCDAs are rigorously defined by the matrix element sandwiched with the quark bilinears with light-cone separation, and then switch to the actual momenta and the near light-like distance x for the practise of phenomenas. In Refs. [24,43,44], high twist LCDAs of vector mesons are systematical studied in QCD based on conformal expansion with taking into account meson and quark mass corrections. The complete analysis of the parameters from QCD sum rules and a renormalon based model are presented in Refs. [22,23]. Considering the polarisation decomposition in Eq. (37) to the vector Dirac structure, the matrix element sandwiched between vacuum and vector meson state takes the following parameterisation

$$
\langle \phi(p, \epsilon) | \bar{s}(x) \gamma_\mu s(0) | 0 \rangle
$$
$$
= f_\phi^\parallel m_\phi \int_0^1 du e^{iup \cdot x} \left\{ \epsilon_\mu \left[\phi_3^\perp(u) + \frac{m_\phi^2 x^2}{16} \phi_5^\perp(u) \right] \right.
$$
$$
+ p_\mu \frac{\epsilon \cdot x}{p \cdot x} \left[\phi_2^\parallel(u) - \phi_3^\perp(u) + \frac{m_\phi^2 x^2}{16} \left(\phi_4^\parallel(u) - \phi_5^\perp(u) \right) \right]
$$
$$
\left. - \frac{(\epsilon \cdot x) m_\phi^2}{2(p \cdot x)^2} x_\mu \left[\psi_4^\parallel(u) - 2\phi_3^\perp(u) + \phi_2^\parallel(u) \right] \right\}, \tag{38}
$$

$$
\langle \phi(p, \epsilon) | \bar{s}(x) \sigma_{\mu\nu} s(0) | 0 \rangle
$$
$$
= -i f_\phi^\perp \int_0^1 du e^{iup \cdot x} \left\{ (\epsilon_\mu p_\nu - \epsilon_\nu p_\mu) \left[\phi_2^\perp(u) + \frac{m_\phi^2 x^2}{16} \phi_4^\perp(u) \right] \right.
$$
$$
+ (p_\mu x_\nu - p_\nu x_\mu) \frac{(\epsilon \cdot x) m_\phi^2}{(p \cdot x)^2} \left[\phi_3^\parallel(u) - \frac{1}{2}\phi_2^\perp(u) - \frac{1}{2}\psi_4^\perp(u) \right]
$$
$$
\left. + \frac{m_\phi^2}{2(p \cdot x)} (\epsilon_\mu x_\nu - \epsilon_\nu x_\mu) \left[\psi_4^\perp(u) - \phi_2^\perp(u) \right] \right\}, \tag{39}
$$

$$
\langle \phi(p, \epsilon) | \bar{s}(x) \gamma_\mu \gamma_5 s(0) | 0 \rangle
$$
$$
= -\frac{f_\phi^\parallel m_\phi \varepsilon_{\mu\nu\rho\sigma} \epsilon^{*\nu} p^\rho x^\sigma}{4} \int_0^1 du e^{iup \cdot x}
$$
$$
\cdot \left[\tilde{\psi}_3^\perp(u) + \frac{m_\phi^2 x^2}{16} \tilde{\psi}_5^\perp(u) \right], \tag{40}
$$

$$
\langle \phi(p, \epsilon) | \bar{s}(x) s(0) | 0 \rangle = -\frac{i}{2} f_\phi^\perp (\epsilon \cdot x) m_\phi^2 \int_0^1 du e^{iup \cdot x} \tilde{\psi}_3^\parallel(u). \tag{41}
$$

We use the conventions

$$
\varepsilon_{0123} = -\varepsilon^{0123} = 1, \quad \gamma_5 = \frac{i}{4!} \varepsilon^{\mu\nu\rho\sigma} \gamma_\mu \gamma_\nu \gamma_\rho \gamma_\sigma. \tag{42}
$$

The quark mass effects are taken into account in the last two parameterisations of matrix elements with the Dirac struc-

tures $\gamma_\mu \gamma_5$ and **1**, and the auxillary DAs read as

$$
\tilde{\psi}_3^\parallel(u) = \left(1 - r_\parallel \delta_+\right) \psi_3^\parallel(u),
$$
$$
\tilde{\psi}_{3(5)}^\perp(u) = (1 - r_\perp \delta_+) \psi_{3(5)}^\perp(u), \tag{43}
$$

with $r_\parallel = f_\phi^\parallel / f_\phi^\perp$, $r_\perp = f_\phi^\perp / f_\phi^\parallel$ and $\delta_\pm = (m_s \pm m_s)/m_\phi$. The DAs $\phi = \{\phi_2^{\parallel(\perp)}, \phi_3^{\parallel(\perp)}, \psi_3^\parallel, \psi_4^{\parallel(\perp)}\}$ satisfy the normalisations

$$
\int_0^u \phi(u')du'\Big|_{u=1} = 1, \quad \int_0^u du' \int_0^{u'} \phi(u'')du''\Big|_{u=1} = 1 \tag{44}
$$

and also the equation of motions (EOM) of the LCDAs. The DAs $\phi' = \{\phi_4^{\parallel(\perp)}, \phi_5^\perp, \psi_5^\perp\}$ are not subject to a particular normalisation while $\int_0^u du' \left(\phi_4^\parallel - \phi_5^\perp\right)\big|_{u=1} = 0$ is necessary, and they relates to DAs ϕ, at first order of $\mathcal{O}(m_\phi^2)$ expansion, by [44]

$$
\phi_4^\parallel(u) = -4 \int_0^u \left[(2u' - 1)\phi_2^\parallel(u') \right]
$$
$$
+ 4 \int_0^u du' \int_0^{u'} du'' \left[\phi_3^\perp(u'') - \psi_4^\parallel(u'') - 3\phi_2^\parallel(u'') \right],
$$
$$
\phi_4^\perp(u) = -4 \int_0^u \left[(2u' - 1)\phi_2^\perp(u') \right]
$$
$$
+ 4 \int_0^u du' \int_0^{u'} du'' \left[\psi_4^\perp(u'') - \phi_2^\perp(u'') \right],
$$
$$
\phi_5^\perp(u) = -4 \int_0^u \left[(2u' - 1)\phi_3^\perp(u') \right],
$$
$$
\psi_5^\perp(u) = -4 \int_0^u \left[(2u' - 1)\psi_3^\perp(u') \right]. \tag{45}
$$

We notice that the last two relation equations hold only for asymptotic LCDAs [24].

The lower twists DAs are conventionally expanded in conformal spin which is analogous to the partial wave expansion of SO(3), and write in terms of Gegenbauer polynomials with corresponding moments. In this work we take the truncation to the second order of leading twist DAs expansion,

$$
\phi_2^{\parallel(\perp)}(u) = 6u(1 - u) \left[1 + a_1^{\parallel(\perp)} C_1^{3/2}(t) + a_2^{\parallel(\perp)} C_2^{3/2}(t) \right]. \tag{46}
$$

The twist 3 DAs contributed from the leading twist DAs are cited as [43]

$$
\phi_3^\parallel(u) = \frac{1}{2} \int_0^u du' \frac{\Psi_2^\parallel(u')}{\bar{u}'} + \frac{1}{2} \int_u^1 du' \frac{\Psi_2^\parallel(u')}{u'},
$$
$$
\tilde{\psi}_3^\parallel(u) = \bar{u} \int_0^u du' \frac{\Psi_2^\parallel(u')}{\bar{u}'} + u \int_u^1 du' \frac{\Psi_2^\parallel(u')}{u'},
$$
$$
\phi_3^\perp(u) = \frac{1}{4} \int_0^u du' \frac{\Psi_2^\perp(u')}{\bar{u}'} + \frac{1}{4} \int_u^1 du' \frac{\Psi_2^\perp(u')}{u'},
$$
$$
\tilde{\psi}_3^\perp(u) = \bar{u} \int_0^u du' \frac{\Psi_2^\perp(u')}{\bar{u}'} + u \int_u^1 du' \frac{\Psi_2^\perp(u')}{u'}, \tag{47}
$$

Table 4 Notations of the LCDAs of light vector mesons (up tabular) and nonperturbative parameters at the factorization scale $\mu_f = 1.66\,\text{GeV}$ of the ϕ meson LCDAs taken in our evaluation (low tabular)

Notations	$\phi_2^{\parallel}$	$\phi_2^{\perp}$	$\phi_3^{\parallel}$	$\psi_3^{\parallel}$	$\phi_3^{\perp}$	$\psi_3^{\perp}$	$\phi_4^{\parallel}$	$\psi_4^{\parallel}$	$\phi_4^{\perp}$	$\psi_4^{\perp}$	$\phi_5^{\perp}$	$\psi_5^{\perp}$
Twist	2	2	3	3	3	3	4	4	4	4	5	5
Dirac	γ_μ	$\sigma_{\mu\nu}$	$\sigma_{\mu\nu}$	$\mathbf{1}$	γ_μ	$\gamma_\mu\gamma_5$	γ_μ	γ_μ	$\sigma_{\mu\nu}$	$\sigma_{\mu\nu}$	γ_μ	$\gamma_\mu\gamma_5$
Expressions	(46)	(46)	(47)	(47)	(47)	(47)	(54)	(53)	(54)	(53)	(54)	(54)
Para.	$\bar{m}_s$(GeV)	m_ϕ(GeV)	$f_\phi^{\parallel}$(GeV)	$f_\phi^{\perp}$(GeV)	$a_1^{\parallel(\perp)}$	$a_2^{\parallel}$	$a_2^{\perp}$					
Value	0.101(8)	1.68	0.233(4)	0.184(4)	0	0.243(80)	0.148(70)					

with the auxiliary functions

$$\Psi_2^{\parallel}(u') = 2\phi_2^{\perp}(u') + r_{\parallel}\left[\frac{(3-2u')}{2}\delta_+ + \frac{\delta_-}{2}\right]\frac{\partial\phi_2^{\perp}(u')}{\partial u'},$$

$$\Psi_2^{\perp}(u') = 2\phi_2^{\parallel}(u') + r_{\perp}\left[\delta_+(2u'-1) + \delta_-\right]\frac{\partial\phi_2^{\perp}(u')}{\partial u'}. \tag{48}$$

We here present their explicit expressions truncated to the second term of gegenbauer polynormias of $\phi_2^{\parallel/\perp}(u)$

$$\phi_3^{\parallel}(u) = 3 - 6u + 6u^2$$
$$+ \frac{3r_{\parallel}}{2}\delta_+\left[-6 + 12u - 4u^2 + \log(1-u) - 3\log u\right]$$
$$+ a_2^{\perp}(\mu)\left[3(1 - 12u + 42u^2 - 60u^3 + 30u^4)\right]$$
$$+ a_2^{\perp}(\mu)3r_{\parallel}\delta_+\left[-33 + 126u - 222u^2 + 200u^3\right.$$
$$\left. - 60u^4 + 3\log(1-u) - 9\log u\right], \tag{49}$$

$$\tilde{\psi}_3^{\parallel}(u) = 2(1-u)\left[3 - 6u + 6u^2\right.$$
$$+ \frac{3r_{\parallel}}{2}\delta_+(-6 + 12u - 4u^2 + \log(1-u) - 3\log u)\right]$$
$$+ a_2^{\perp}(\mu)6u\left[1 - 12u + 42u^2 - 60u^3 + 30u^4\right]$$
$$+ a_2^{\perp}(\mu)6ur_{\parallel}\delta_+\left[-33 + 126u - 222u^2 + 200u^3\right.$$
$$\left. - 60u^4 + 3\log(1-u) - 9\log u\right], \tag{50}$$

$$\phi_3^{\perp}(u) = \frac{1}{2}\left\{3 - 6u + 6u^2\right.$$
$$+ 3r_{\perp}\delta_+\left[2 - 4u + 4u^2 + \log(1-u) + \log u\right]$$
$$+ a_2^{\parallel}(\mu)3\left[1 - 12u + 42u^2 - 60u^3 + 30u^4\right]$$
$$+ a_2^{\perp}(\mu)6r_{\perp}\delta_+\left[11 - 42u + 102u^2 - 120u^3\right.$$
$$\left. + 60u^4 + 3\log(1-u) + 3\log u\right]\right\}, \tag{51}$$

$$\tilde{\psi}_3^{\perp}(u) = 2(1-u)\left[3 - 6u + 6u^2\right.$$
$$+ 3r_{\perp}\delta_+(2 - 4u + 4u^2 + \log(1-u) + \log u)\right]$$
$$+ a_2^{\parallel}(\mu)6u\left[1 - 12u + 42u^2 - 60u^3 + 30u^4\right]$$
$$+ a_2^{\perp}(\mu)12ur_{\perp}\delta_+\left[11 - 42u + 102u^2 - 120u^3\right.$$

$$\left. + 60u^4 + 3\log(1-u) + 3\log u\right]. \tag{52}$$

In the asymptotic limit, the twist 4 DAs contributed at the order $\mathcal{O}((p\cdot x)^{-2})$ are given by

$$\psi_4^{\parallel}(u) = 6u\bar{u}, \qquad \psi_4^{\perp}(u) = 6u\bar{u}, \tag{53}$$

the twist 4 and twist 5 DAs ϕ' contributed at the order $\mathcal{O}(m_\phi^2 x^2)$ read from Eq. (45) as

$$\phi_4^{\parallel}(u) = 24u^2\bar{u}^2, \quad \phi_4^{\perp}(u) = 24u^2\bar{u}^2,$$
$$\phi_5^{\perp}(u) = 6u\bar{u}(1 - u\bar{u}), \quad \psi_5^{\perp}(u) = 12u^2\bar{u}^2. \tag{54}$$

For the sake of convenient we list the DAs at different twists with corresponding Dirac structures in Table 4, and also we present the nonperturbaive parameters of LCDAs taken in our evaluation. The mass of ϕ meson and strange quark in the $\overline{\text{MS}}$ scheme are taken from PDG [1]. The longitudinal decay constant $f_\phi^{\parallel}$ is mainly determined directly by the experiment measurement of channel $e^+e^- \to \phi(\to PP)$ [24], the scale dependent transversal decay constant is chosen by considering the ratio $r_{\perp}(1\,\text{GeV}) = f_\phi^{\perp}(1\,\text{GeV})/f_\phi^{\parallel} = 0.820$ obtained from lattice QCD simulated by using $N_f = 2 + 1$ domain-wall fermions at the spacing $a = 0.114\,\text{fm}$ and masses down to $m_\pi = 330\,\text{MeV}$ [45]. The Gegenbauer moments $a_2^{\parallel(\perp)}$ are taken from Ref. [46] where a combined analysis is performed on the lattice simulation and QCD sum rule calculation [47].

B Imaginary part of OPE invariant amplitudes

In the case of transversal helicity with longitudinal leptonic current and transversal ϕ meson, the imaginary part of OPE invariant amplitudes are

$$\frac{1}{\pi}\text{Im}F_{1,0\pm}^{\text{OPE}}(q^2 < 0, u)$$

$$= \left[\frac{\sqrt{\lambda}}{2\sqrt{|q^2|}} \pm \frac{\left(m_{D^*}^2 - m_\phi^2 - q^2\right)}{2\sqrt{|q^2|}}\right]m_c f_\phi^{\perp}\phi_2^{\perp}(u)$$

$$+ \left[\frac{u\sqrt{\lambda}}{2\sqrt{|q^2|}} \pm \frac{u\left(m_{D^*}^2 - m_\phi^2 - q^2\right) + 2q^2}{2\sqrt{|q^2|}}\right]f_\phi^{\parallel}m_\phi\phi_3^{\perp}(u)$$

$$+\left[-\frac{\sqrt{\lambda}}{2\sqrt{|q^2|}}\pm\frac{\left(m_{D_s^*}^2-m_\phi^2-q^2\right)}{2\sqrt{|q^2|}}\right]f_\phi^\parallel m_\phi\left(\bar\phi_2^\parallel(u)-\bar\phi_3^\perp(u)\right)$$

$$+\frac{\sqrt{\lambda}}{4\sqrt{|q^2|}}f_\phi^\parallel m_\phi\tilde\psi_3^\perp(u),\tag{55}$$

$$\frac{1}{\pi}\mathrm{Im}F_{2,0\pm}^{\mathrm{OPE}}(q^2<0,u)$$

$$=\left[\frac{\sqrt{\lambda}\left[u\left(m_{D_s^*}^2-m_\phi^2-q^2\right)+2q^2\right]}{2\sqrt{|q^2|}}\pm\frac{u\lambda}{2\sqrt{|q^2|}}\right]$$

$$\cdot\left[\frac{f_\phi^\parallel m_\phi\tilde\psi_3^\perp(u)}{4}\mp\frac{f_\phi^\parallel m_\phi^3\phi_5^\perp(u)}{4\sqrt{\lambda}}\right.$$

$$\left.\mp\frac{m_c f_\phi^\perp m_\phi^2\left(\bar\psi_4^\perp(u)-\bar\phi_2^\perp(u)\right)}{\sqrt{\lambda}}\right]$$

$$-\frac{u\sqrt{\lambda}}{\sqrt{|q^2|}}f_\phi^\parallel m_\phi^3\left(\bar{\bar\psi}_4^\parallel(u)+\bar{\bar\phi}_2^\parallel(u)-2\bar{\bar\phi}_3^\perp(u)\right)$$

$$+\left[\frac{\sqrt{\lambda}}{8\sqrt{|q^2|}}\mp\frac{\left(m_{D_s^*}^2-m_\phi^2-q^2\right)}{8\sqrt{|q^2|}}\right]f_\phi^\parallel m_\phi^3\left(\bar\phi_4^\parallel(u)-\bar\phi_5^\perp(u)\right)$$

$$-\frac{\sqrt{\lambda}}{16\sqrt{|q^2|}}f_\phi^\parallel m_\phi^3\tilde\psi_5^\perp(u)+\left[\frac{\sqrt{\lambda}}{2\sqrt{|q^2|}}\pm\frac{\left(m_{D_s^*}^2-m_\phi^2-q^2\right)}{2\sqrt{|q^2|}}\right]$$

$$\cdot f_\phi^\perp m_\phi^2 m_c\left(\bar{\bar\psi}_4^\perp(u)+\bar{\bar\phi}_2^\perp(u)-2\bar{\bar\phi}_3^\parallel(u)\right),\tag{56}$$

$$\frac{1}{\pi}\mathrm{Im}F_{3,0\pm}^{\mathrm{OPE}}(q^2<0,u)$$

$$=\left[-\frac{\sqrt{\lambda}}{4\sqrt{|q^2|}}\mp\frac{\left(m_{D_s^*}^2-m_\phi^2-q^2\right)}{4\sqrt{|q^2|}}\right]m_c^3 f_\phi^\perp m_\phi^2\phi_4^\perp(u)$$

$$+\left[-\frac{u\sqrt{\lambda}}{4\sqrt{|q^2|}}\mp\frac{u\left(m_{D_s^*}^2-m_\phi^2-q^2\right)+2q^2}{4\sqrt{|q^2|}}\right]m_c^2 f_\phi^\parallel m_\phi^3\phi_5^\perp(u)$$

$$+\left[-\frac{\sqrt{\lambda}\left[2m_c^2+u\left(m_{D_s^*}^2-m_\phi^2-q^2\right)+2q^2\right]}{16\sqrt{|q^2|}}\mp\frac{u\lambda}{16\sqrt{|q^2|}}\right]$$

$$\cdot f_\phi^\parallel m_\phi^3\tilde\psi_5^\perp(u)$$

$$+\left[\frac{\sqrt{\lambda}}{4\sqrt{|q^2|}}\mp\frac{\left(m_{D_s^*}^2-m_\phi^2-q^2\right)}{4\sqrt{|q^2|}}\right]f_\phi^\parallel m_\phi^3 m_c^2\left(\bar\phi_4^\parallel(u)-\bar\phi_5^\perp(u)\right).$$

$$\tag{57}$$

The imaginary parts of OPE invariant amplitudes with transversal leptonic and longitudinal ϕ currents are

$$\frac{1}{\pi}\mathrm{Im}F_{1,\pm0}^{\mathrm{OPE}}(q^2<0,u)$$

$$=\mp f_\phi^\perp m_c m_\phi\phi_2^\perp(u)\mp f_\phi^\parallel m_\phi^2\left(\bar\phi_2^\parallel(u)-\bar\phi_3^\perp(u)\right)$$

$$+\left[\sqrt{\lambda}\mp\left(m_{D_s^*}^2-m_\phi^2-q^2+2um_\phi^2\right)\right]\frac{f_\phi^\parallel}{2}\phi_3^\perp(u),\tag{58}$$

$$\frac{1}{\pi}\mathrm{Im}F_{2,\pm0}^{\mathrm{OPE}}(q^2<0,u)$$

$$=-\left[\sqrt{\lambda}\left(m_{D_s^*}^2-m_\phi^2-q^2+2um_\phi^2\right)\mp\lambda\right]$$

$$\cdot\frac{f_\phi^\parallel}{2}\left(\bar\phi_2^\parallel(u)-\bar\phi_3^\perp(u)\right)$$

$$-\left[\sqrt{\lambda}\mp\left(m_{D_s^*}^2-m_\phi^2-q^2+2um_\phi^2\right)\right]\frac{f_\phi^\parallel m_\phi^2}{8}\phi_5^\perp(u)$$

$$-2f_\phi^\parallel m_\phi^2\sqrt{\lambda}\left(\bar{\bar\psi}_4^\parallel(u)+\bar{\bar\phi}_2^\parallel(u)-2\bar{\bar\phi}_3^\perp(u)\right)$$

$$\mp f_\phi^\perp m_c m_\phi^3\left(\bar{\bar\psi}_4^\perp(u)+\bar{\bar\phi}_2^\perp(u)-2\bar{\bar\phi}_3^\parallel(u)\right)$$

$$\pm\left(m_{D_s^*}^2-m_\phi^2-q^2+2um_\phi^2\right)\frac{f_\phi^\perp m_c m_\phi}{2}\left(\bar\psi_4^\perp(u)-\bar\phi_2^\perp(u)\right)$$

$$+\frac{f_\phi^\perp m_\phi m_c}{2}\sqrt{\lambda}\,\tilde\psi_3^\perp(u)\pm\frac{f_\phi^\parallel m_\phi^4}{4}\left(\bar\phi_4^\parallel(u)-\bar\phi_5^\perp(u)\right),\tag{59}$$

$$\frac{1}{\pi}\mathrm{Im}F_{3,\pm0}^{\mathrm{OPE}}(q^2<0,u)$$

$$=\left[\sqrt{\lambda}\left(m_{D_s^*}^2-m_\phi^2-q^2+2um_\phi^2\right)\mp\lambda\pm2m_c^2 m_\phi^2\right]$$

$$\cdot\frac{f_\phi^\parallel m_\phi^2}{4}\left(\bar\phi_4^\parallel(u)-\bar\phi_5^\perp(u)\right)$$

$$-2f_\phi^\parallel m_\phi^2\sqrt{\lambda}\left(um_{D_s^*}^2+\bar u q^2-u\bar u m_\phi^2\right)$$

$$\cdot\left(\bar{\bar\psi}_4^\parallel(u)+\bar{\bar\phi}_2^\parallel(u)-2\bar{\bar\phi}_3^\perp(u)\right)$$

$$\pm\frac{f_\phi^\perp m_c^3 m_\phi^3}{2}\phi_4^\perp(u)\pm f_\phi^\perp m_\phi m_c\lambda\left(\bar{\bar\psi}_4^\perp(u)+\bar{\bar\phi}_2^\perp(u)-2\bar{\bar\phi}_3^\parallel(u)\right)$$

$$-\left[\sqrt{\lambda}\mp\left(m_{D_s^*}^2-m_\phi^2-q^2+2um_\phi^2\right)\right]\frac{f_\phi^\parallel m_\phi^2 m_c^2}{4}\phi_5^\perp(u).\tag{60}$$

For the transversal helicity form factor, the imaginary parts are

$$\frac{1}{\pi}\mathrm{Im}F_{1,\pm\mp}^{\mathrm{OPE}}(q^2<0,u)$$

$$=\left[\frac{\bar u\sqrt{\lambda}}{2m_{D_s^*}}\pm\frac{\left((1+u)m_{D_s^*}^2-\bar u m_\phi^2+\bar u q^2\right)}{2m_{D_s^*}}\right]f_\phi^\parallel m_\phi\phi_3^\perp(u)$$

$$+\left[\frac{\sqrt{\lambda}}{2m_{D_s^*}}\pm\frac{\left(m_{D_s^*}^2+m_\phi^2-q^2\right)}{2m_{D_s^*}}\right]$$

$$\cdot\left[f_\phi^\perp m_c\phi_2^\perp(u)+f_\phi^\perp m_\phi\left(\bar\phi_2^\parallel(u)-\bar\phi_3^\perp(u)\right)\right]$$

$$+\frac{\sqrt{\lambda}}{4m_{D_s^*}}f_\phi^\parallel m_\phi\tilde\psi_3^\perp(u),\tag{61}$$

$$\frac{1}{\pi}\mathrm{Im}F_{2,\pm\mp}^{\mathrm{OPE}}(q^2<0,u)$$

$$=\left[\frac{\left((1+u)m_{D_s^*}^2-\bar u m_\phi^2+\bar u q^2\right)\sqrt{\lambda}}{2m_{D_s^*}}\pm\frac{\bar u\lambda}{2m_{D_s^*}}\right]$$

$$\cdot\left[\frac{f_\phi^\parallel m_\phi\tilde\psi_3^\perp(u)}{4}\mp\frac{f_\phi^\parallel m_\phi^3\phi_5^\perp(u)}{4\sqrt{\lambda}}\right.$$

$$\left.\mp\frac{f_\phi^\perp m_\phi^2 m_c\left(\bar\psi_4^\perp(u)-\bar\phi_2^\perp(u)\right)}{\sqrt{\lambda}}\right]$$

$$+\left[\frac{\sqrt{\lambda}}{2m_{D_s^*}}\pm\frac{\left(m_{D_s^*}^2+m_\phi^2-q^2\right)}{2m_{D_s^*}}\right]$$

$$\cdot \left[f_\phi^\perp m_\phi^2 m_c \left(\overset{=}{\psi_4^\perp}(u) + \overset{=}{\phi_2^\perp}(u) - 2\overset{=}{\phi_3^\parallel}(u) \right) \right.$$

$$\left. - \frac{f_\phi^\parallel m_\phi^3 \left(\bar{\phi}_4^\parallel(u) - \bar{\phi}_5^\perp(u) \right)}{4} \right]$$

$$- \frac{\bar{u}\sqrt{\lambda}}{m_{D_s^*}} f_\phi^\parallel m_\phi^3 \left(\overset{=}{\psi_4^\parallel}(u) + \overset{=}{\phi_2^\parallel}(u) - 2\overset{=}{\phi_3^\perp}(u) \right)$$

$$- \frac{\sqrt{\lambda}}{16 m_{D_s^*}} f_\phi^\parallel m_\phi^3 \tilde{\psi}_5^\perp(u), \tag{62}$$

$$\frac{1}{\pi} \operatorname{Im} F_{3,\pm\mp}^{\text{OPE}}(q^2 < 0, u)$$

$$= \left[-\frac{\bar{u}\sqrt{\lambda}}{4 m_{D_s^*}} \mp \frac{\left((1+u)m_{D_s^*}^2 - \bar{u}m_\phi^2 + \bar{u}q^2 \right)}{4 m_{D_s^*}} \right] f_\phi^\parallel m_\phi^3 m_c^2 \, \phi_5^\perp(u)$$

$$- \left[\frac{\left(2m_c^2 + (1+u)m_{D_s^*}^2 - \bar{u}m_\phi^2 + \bar{u}q^2 \right) \sqrt{\lambda}}{16 m_{D_s^*}} \pm \frac{\bar{u}\lambda}{16 m_{D_s^*}} \right]$$

$$\cdot f_\phi^\parallel m_\phi^3 \, \tilde{\psi}_5^\perp(u)$$

$$- \left[\frac{\sqrt{\lambda}}{4 m_{D_s^*}} \pm \frac{\left(m_{D_s^*}^2 + m_\phi^2 - q^2 \right)}{4 m_{D_s^*}} \right]$$

$$\cdot \left[f_\phi^\perp m_\phi^2 m_c^3 \, \phi_4^\perp(u) + f_\phi^\parallel m_\phi^3 m_c^2 \left(\bar{\phi}_4^\parallel(u) - \bar{\phi}_5^\perp(u) \right) \right]. \tag{63}$$

References

1. R.L. Workman et al., (Particle Data Group), Prog. Theor. Exp. Phys **2022**, 083C01 (2022)
2. M. Neubert, Phys. Rept. **245**, 259–396 (1994)
3. Q. Qin, Y.F. Shen, F.S. Yu, Chin. Phys. C **45**(10), 103106 (2021)
4. Q. Qin, Y.J. Shi, W. Wang, G.H. Yang, F.S. Yu, R. Zhu, Phys. Rev. D **105**(3), L031902 (2022)
5. N. Isgur, M.B. Wise, Phys. Lett. B **232**, 113–117 (1989)
6. S. Nussinov, W. Wetzel, Phys. Rev. D **36**, 130 (1987)
7. M.B. Voloshin, M.A. Shifman, Sov. J. Nucl. Phys. **45**, 292 (1987)
8. M.B. Voloshin, M.A. Shifman, Yad. Fiz. **45**, 463 (1987)
9. G.C. Donald, C.T.H. Davies, J. Koponen, G.P. Lepage, Phys. Rev. Lett. **112**, 212002 (2014)
10. H.D. Li, C.D. Lü, C. Wang, Y.M. Wang, Y.B. Wei, JHEP **04**, 023 (2020)
11. B. Pullin, R. Zwicky, JHEP **09**, 023 (2021)
12. P. Ball, V.M. Braun, H.G. Dosch, Phys. Rev. D **44**, 3567–3581 (1991)
13. A. Khodjamirian, R. Ruckl, S. Weinzierl, C.W. Winhart, O.I. Yakovlev, Phys. Rev. D **62**, 114002 (2000)
14. P. Ball, Phys. Lett. B **641**, 50–56 (2006)
15. N. Offen, F.A. Porkert, A. Schäfer, Phys. Rev. D **88**(3), 034023 (2013)
16. I. Bediaga, M. Nielsen, Phys. Rev. D **68**, 036001 (2003)
17. D.S. Du, J.W. Li, M.Z. Yang, Eur. Phys. J. C **37**(2), 173–184 (2004)
18. Y.L. Wu, M. Zhong, Y.B. Zuo, Int. J. Mod. Phys. A **21**, 6125–6172 (2006)
19. C. Bourrely, I. Caprini, L. Lellouch, Phys. Rev. D **79**, 013008 (2009) [erratum: Phys. Rev. D **82**, 099902 (2010)]
20. D. Becirevic, A.B. Kaidalov, Phys. Lett. B **478**, 417–423 (2000)
21. P. Ball, R. Zwicky, Phys. Rev. D **71**, 014029 (2005)
22. P. Ball, G.W. Jones, JHEP **03**, 069 (2007)
23. P. Ball, V.M. Braun, A. Lenz, JHEP **08**, 090 (2007)
24. A. Bharucha, D.M. Straub, R. Zwicky, JHEP **08**, 098 (2016)
25. Y.M. Wang, H. Zou, Z.T. Wei, X.Q. Li, C.D. Lu, Eur. Phys. J. C **54**, 107–121 (2008)
26. Q. Chang, L.T. Wang, X.N. Li, JHEP **12**, 102 (2019)
27. G. Hiller, R. Zwicky, JHEP **03**, 042 (2014)
28. J. Gratrex, M. Hopfer, R. Zwicky, Phys. Rev. D **93**(5), 054008 (2016)
29. G. Hiller, R. Zwicky, JHEP **11**, 073 (2021)
30. G.P. Lepage, S.J. Brodsky, Phys. Rev. D **22**, 2157 (1980)
31. A.V. Efremov, A.V. Radyushkin, Phys. Lett. B **94**, 245–250 (1980)
32. V.L. Chernyak, A.R. Zhitnitsky, Phys. Rept. **112**, 173 (1984)
33. Y. S. Amhis et al. [HFLAV], Eur. Phys. J. C **81**(3), 226 (2021)
34. M. Ablikim et al. [BESIII], Phys. Rev. Lett. **123**(21), 211802 (2019)
35. M. Ablikim et al. [BESIII], Phys. Rev. Lett. **121**(17), 171803 (2018)
36. G. Buchalla, A.J. Buras, M.E. Lautenbacher, Rev. Mod. Phys. **68**, 1125–1144 (1996)
37. Y. Yang, K. Li, Z. Li, J. Huang, J. Sun., Eur. Phys. J. C **82**(6), 555 (2022)
38. E. Kou et al. [Belle-II], PTEP **2019**(12), 123C01 (2019) [erratum: PTEP **2020**, no.2, 029201 (2020)]
39. D_s^+ reconstruction plots - The Belle II Collaboration et al - BELLE2-NOTE-PL-2020-016, https://docs.belle2.org/record/2039/files/BELLE2-NOTE-PL-2020-016.pdf
40. Y. Guan et al., Belle. Phys. Rev. D **103**, 112005 (2021)
41. M. Ablikim et al. [BESIII], Chin. Phys. C **44**(4), 040001 (2020)
42. R. Aaij et al., LHCb. JHEP **12**, 144 (2020)
43. P. Ball, V.M. Braun, Y. Koike, K. Tanaka, Nucl. Phys. B **529**, 323–382 (1998)
44. P. Ball, V.M. Braun, Nucl. Phys. B **543**, 201–238 (1999)
45. C. Allton et al., RBC-UKQCD. Phys. Rev. D **78**, 114509 (2008)
46. M. Dimou, J. Lyon, R. Zwicky, Phys. Rev. D **87**(7), 074008 (2013)
47. R. Arthur, P.A. Boyle, D. Brommel, M.A. Donnellan, J.M. Flynn, A. Juttner, T.D. Rae, C.T.C. Sachrajda, Phys. Rev. D **83**, 074505 (2011)